September 2013

Evaporation in a Binary Liquid Falling Film

Ye Lu
Worcester Polytechnic Institute

Evaporation in a Binary Liquid Falling Film

A Major Qualifying Project
Submitted to the Faculty of
Worcester Polytechnic Institute
in partial fulfillment of the requirements for the
Degree in Bachelor of Science
in
Mathematical Sciences
By

Ye Lu

Date: September 9, 2013

Approved:

Professor B.S. Tilley, Advisor

Keywords:
1. Evaporation
2. Thin film

Abstract

Thin liquid films are ubiquitous in both nature and industrial applications, such as tear films and coating process. Understanding the mechanism of the thin liquid films becomes important so that we can predict on their dynamics and stabilities. In this project, we will focus on the stability and dynamics of a fluid film of two miscible liquids falling along an inclined plane with one fluid component is evaporating at the free surface. We utilize Navier-Stokes equation for incompressible Newtonian fluids, heat equation for energy balance and vapor-liquid jump conditions for mass balance at the free boundary. We then non-dimensionalize the system and apply perturbation theory to simplify the system to obtain two evolution equations for film and concentration respectively. With an initially flat film, a variation in the concentration field results in a wave pattern in the film profile. As the film travels, the film profile overlaps with the concentration profile, and three types of sharp transitions will occur in the film profile: a. the film peak speeds up and moves forward, b. the film peak moves backward and then moves forward again, c. film will be slowed down and two local peaks will form in the film.

Acknowledgements

I would like to express my very great appreciation to my project advisor, Professor Burt S. Tilley, without whom this project would not have been possible. His consistent support, guidance and patience have been a great help for me throughout the project, even when sometimes I don't deserve it. Thanks for not giving up on me!

Contents

Chapter 1

Background

Thin liquid films appear widely in nature and in industrial processes, and they have a wide variety of roles. Gravity currents such as a sea-breeze front, which when fluid of one density flows horizontally into fluid of a different density[1]. Tear films, which protects the eye with bactericidal enzymes and provides an optically smooth surface for light refraction are thin liquid films [2]. More commonly, motor oil, which protects moving parts in engines from friction wear to increase endurance also appear as thin liquid films [3]. More examples includes thin film coating, magnetic films in memory device and among many other applications for heat and mass transfer [4].

The interface between the liquid and the surrounding gas is a deformable boundary, these films display wave motions. In 2D thin films, the unstable structure includes increased wave amplitude as it travels. One example of the instability is that as the film travels, different forces acting on and within the fluid will cause the film to rupture, in which the substrate will be exposed to the ambient gas [5]. For certain situation rupture needs to be avoided such as during painting. Some interesting phenomena occurs when temperature variation is introduced in the film because temperature changes surface tension which will change the dynamics of the free surface. With localized heating, a falling film may form a horizontal band at the upper edge of the heater due to the surface tension gradient [6]. Also heating can induce mass flows on the free surface in means of evaporation(condensation). A result from [12] shows that, the film will eventually rupture, but with thermocapillary effect, the time for the rupture to form will be lengthened during evaporation. Also there are studies investigating 3D falling films and related experiments were conducted. As the film flows down in 3D plane, the film front develops a series of fingers across the slope and distances between neighboring fingers are relatively the same [5]. As the dynamics of the thin film varies with conditions, in order to better predict the stability and dynamics of thin liquid films, we need to first understand the physics associated with thin films.

The scale of thin films varies from few centimeters in cooling processes of electronic components to tenth of meters in industrial evaporators [7]. Started with the general liquid films, the early study of thin film dynamics is by D.J Benney [8], who studied possible wave motions on a steady 2D laminar flow of single liquid down an inclined plane. He developed a film evolution equation

and many later works has been done based on Benney's work and were often referred to evolution equation derived by Benney. G. J Roskes extended the two-dimensional result from Benney into three-dimensions and investigated the interactions between two- and three-dimensional nonlinear waves formed on liquid film [9]. Following the result by Roskes, Lin and Krishna [10] studied the nonlinear stability of the problem with an initially finite 3D disturbances and they discovered that the film becomes unstable with respect to small disturbances at some critical Reynolds number. Liu et al [11] performed an experimental study based on the previous theoretical results, on the instabilities of both 2D and 3D flows down an inclined plane in order to understand the transition to complex disordered patterns and had identified certain three-dimensional instabilities with different Reynolds number and frequency. Since the evolution equation by Benney assumed no mass flux on the free surface, Burelbach et al [12] investigated the effect of mass flux on the stability of a thin liquid layer which is either evaporating or condensing. They had investigated a variety of effects in the study including mass loss(gain), vapor recoil, thermocapillarity, surface tension and viscous forces. Evaporative instabilities were also studied by Hosoi and Bush [13] in which they experimentally investigated the instability of thin film of alcohol-water solution. Then Oron et al systematically investigated the thin liquid film with various settings, for example, bounded films with constant physical properties, free films etc [5]. The study of thin films has still been active and related to many other fields of study. Some of the recent work includes, Cowley-Rosensweig instabilities in a deformable ferrofluid layer in which they included the effect of a weak magnetic field on the thin fluid layer[14], instability of thin film driven by gravity on the outer surface of a cylinder and sphere in which the flow characteristics when pouring down from the top of the cylinder was investigated [15] and many others.

There were studies about evaporating liquid film and also mixture of liquid films, but not much work has been done towards the combination of the two. The problem we will discuss in this report is on the stabilities of a 2-D liquid mixture of two miscible fluids driven by gravity falling down an uniformly heated inclined substrate and bounded above by a passive gas. One liquid component will be evaporating on the free surface.

In the problem, there are two types of diffusion: mass transfer and thermal diffusion. As the differences are small, it's reasonable to assume the linear relation between the mass and heat flux and gradients of temperature and concentration. In a liquid mixture, both types depend on temperature gradient and concentration gradient. The equations are as follows (Note $\boldsymbol{i}$ is mass flux and $\boldsymbol{q}$ is heat flux) [16]:

$$\boldsymbol{i} = -\rho D(\nabla C + \frac{k_\theta}{\theta}\nabla\theta) \tag{1.1}$$

$$\boldsymbol{q} = (k_T \frac{\partial \mu}{\partial C}_{p,\theta} - \theta \frac{\partial \mu}{\partial \theta}_{p,c} + \mu)\boldsymbol{i} - \kappa\nabla\theta \tag{1.2}$$

where μ is an appropriately defined chemical potential for the mixture, D is the diffusion coefficient, C is the concentration, p is the pressure, θ is the temperature, k_p and k_T are pressure and thermal diffusion ratio which provides $k_\theta D$ be the thermal diffusion coefficient and κ is defined as:

$$\kappa = \gamma - \beta^2\theta/\alpha \tag{1.3}$$

where α, β, and γ are coefficients of the potential and temperature gradient:

$$\boldsymbol{i} = -\alpha\nabla\mu - \beta\nabla T, \qquad \boldsymbol{q} = -\beta T\nabla\mu - \gamma\nabla T + \mu\boldsymbol{i} \tag{1.4}$$

Buoyancy-driven convection, also known as natural convection, is generated by density difference within the fluids. There are two primary means of buoyancy-driven convections: one is by temperature gradient and another by concentration gradient. [17]

In the case of temperature-gradient-driven convections, only when the temperature of lower portion of the fluid is higher than that of the upper, does it occur. Fluids near the interface with the plane has higher temperature than ones above and this causes a density gradient and drives the fluids near the interface to move up and thus induces convection within the fluid film. This convection causes heat transfer. Additionally, when the temperature within the liquid is non-uniform, according to kinetic energy theory, the particles who have high temperature move faster than those of low temperature, thus the region of the liquid with higher temperature tend to diffuse into cold region. This phenomenon is known as Soret effect and it can be expressed as in (1.1) that a temperature gradient can induce a diffusive mass flow.

On the free boundary of the film, surface tension is an important force to consider. Surface tension of single liquid depends only on temperature whereas that of mixture of miscible liquids depends on both temperature and concentration. In other words, concentration and temperature gradient in a liquid mixture of miscible fluids will result in surface tension gradient. Since the portion of the liquid with higher surface tension will pull more strongly on the neighboring liquid, it leads fluid motion from region of low surface tension to a region of high surface tension. This effect is known as the Marangoni effect, sometimes also named as thermocapillary convection.

As the differences in temperature and concentration in the problem is small, we propose a linear relation between the surface tension and temperature and concentration [18]

$$\sigma(\theta^*, C) = \sigma_0 - \gamma_\theta(\theta^* - \theta_R) - \gamma_c(C - C_R), \tag{1.5}$$

where γ_θ and γ_c are determined experimentally. With the data in [18], we could calculate the values for both γ at a given temperature and concentration.

In this report, we begin with the study of an isothermal 2-D falling film by Benney [8] in which effects from gravity, interfacial shear stress and capillary are considered. Then in Chapter 3 we will construct a mathematical model for a miscible binary liquid mixture falling along a heated plate and the liquid is evaporating from the free surface. We will apply perturbation theory to get the long wave solution for the model. In order to study the dynamics of the film, we will look at the leading order problem in Chapter 4 and apply linear stability theory to investigate the stability of the film. Then we will study the nonlinear evolution of the film by simulating the film numerically.

Chapter 2

Isothermal Falling Film

In order to understand the modelling progress of a binary thin film, we first discuss the problem of a single liquid falling film without any thermal effect. The film is bounded by a solid surface below and an interface of the liquid and passive gas above. We consider the two-dimensional flow to examine the dynamics of the film thickness where capillary forces and surface shear forces are relevant.

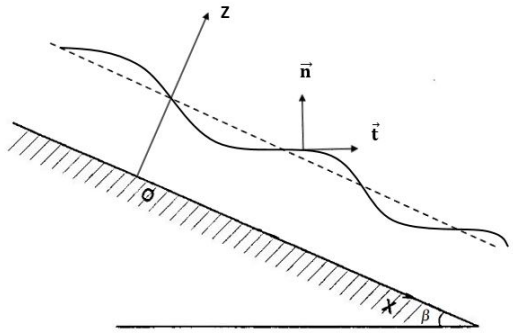

Figure 2.1: A simple falling film

In this chapter we follow the approaches in [8]. The stress tensor of the fluid, normal and tangent vectors on the free surface, and surface tension which is dependent on temperature are defined:

$$\bar{\bar{\boldsymbol{T}}} = -p\boldsymbol{I} + \mu(\nabla\vec{\boldsymbol{u}} + \nabla\vec{\boldsymbol{u}}^{T}), \tag{2.1a}$$

$$\vec{\boldsymbol{n}} = \frac{(-h_x, 1)}{(1+h_x^2)^{1/2}}, \tag{2.1b}$$

$$\vec{\boldsymbol{t}} = \frac{(1, h_x)}{(1+h_x^2)^{1/2}}, \tag{2.1c}$$

The Navier-Stokes and continuity equations for an incompressible fluid are

$$u^*_{x^*} + w^*_{z^*} = 0, \tag{2.2a}$$

$$\rho(u^*_{t^*} + u^* u^*_{x^*} + w^* u^*_{z^*}) = -p^*_{x^*} + \mu\nabla^2 u^* + \rho g^* \sin(\beta), \tag{2.2b}$$

$$\rho(w^*_{t^*} + u^* w^*_{x^*} + w^* w^*_{z^*}) = -p^*_{z^*} + \mu\nabla^2 w^* - \rho g^* \cos(\beta) \tag{2.2c}$$

where $\bar{u}^* = (u^*, w^*)$ is the velocity vector, p^* is the pressure, g^* is the gravity, μ is the viscosity, and ρ is the density.

We assume the no slip boundary conditions at $z^* = 0$:

$$u^* = 0 \qquad\qquad w^* = 0. \tag{2.3}$$

At the free surface $z^* = h^*(x^*, t^*)$, we require the kinematic boundary condition, zero shear stresses, and the normal stress is balanced by capillarity.

$$w^* = h^*_{t^*} + u^* h^*_{x^*}, \tag{2.4a}$$

$$\vec{t} \cdot \bar{\bar{T}} \cdot \vec{n} = 0 \tag{2.4b}$$

$$\vec{n} \cdot \bar{\bar{T}} \cdot \vec{n} = \kappa\sigma \cdot \vec{n} \tag{2.4c}$$

where

$$\kappa = -\nabla \cdot \vec{n} = \frac{h^*_{x^* x^*}}{(1 + h^{*2}_{x^*})^{3/2}}, \tag{2.5}$$

We apply the scaling

$$z = \frac{z^*}{h_0} \qquad x = \frac{x^*}{\lambda} \qquad u = \frac{u^*}{u_0}, \tag{2.6a}$$

$$w = \frac{w^*}{\varepsilon u_0} \qquad t = \frac{u_0 t^*}{\lambda} \qquad p = \frac{h_0 p^*}{\mu u_0} \tag{2.6b}$$

where λ is a characteristic wavelength of the interfatial deformation and the following scaling are used, h_0 is the mean thickness of the film, u_0 is the characteristic velocity

$$u_0 = \frac{h_0^2 \rho g^*}{\mu}, \tag{2.7}$$

$\varepsilon = \frac{h_0}{\lambda}$ is the aspect ratio, which we assume is an asymptotically small perturbation parameter.

From this scaling, we obtain a Reynolds number:

$$Re = \frac{h_0^3 \rho^2 g^*}{\mu^2} = O(1). \tag{2.8}$$

We then apply the scaling to the governing equations and the boundary conditions, the scaled governing system is obtained as

$$u_x + w_z = 0. \tag{2.9a}$$

$$\varepsilon Re(u_t + uu_x + wu_z) = -\varepsilon p_x + u_z z + \varepsilon^2 u_{xx} + \sin\beta, \tag{2.9b}$$

$$\varepsilon^3 Re(w_t + uw_x + ww_z) = -p_z + \varepsilon^2 w_{zz} + \varepsilon^4 w_{xx} - \cos\beta, \tag{2.9c}$$

At $z = 0$, we require the no-slip boundary condition

$$u = 0 \qquad\qquad w = 0. \tag{2.10}$$

At $z = h$, we have the kinematic boundary condition and the balance of shear and normal components of the stress

$$w = h_t + uh_x, \tag{2.11a}$$

$$(u_z + \varepsilon^2 w_x)[1 - \varepsilon^2 h_x^2] - 4\varepsilon^2 h_x u_x = \varepsilon S^{-1}[1 + \varepsilon^2 h_x^2]^{1/2}, \tag{2.11b}$$

$$-p + \frac{2\varepsilon^2}{1 + \varepsilon^2 h_x^2}\{u_x[\varepsilon^2 h_x^2 - 1] - h_x[u_z + \varepsilon^2 w_x]\} = \frac{S^{-1}\varepsilon^3 h_{xx}}{[1 + \varepsilon^2 h_x^2]^{3/2}} \tag{2.11c}$$

where Re is the Reynolds number and S is the capillary number

$$h = \frac{h^*}{h_0} \qquad\qquad S = \frac{u_0 \mu}{\sigma}. \tag{2.12a}$$

We rewrite (2.11a) using (2.9a) to find that

$$h_t + \partial_x \int_0^h u \, dz = 0. \tag{2.13}$$

Now we seek the solution of the governing equations as a perturbation series in power of ε

$$u = u_0 + \varepsilon u_1 + \varepsilon^2 u_2 + ..., \tag{2.14a}$$

$$w = w_0 + \varepsilon w_1 + \varepsilon^2 w_2 + ..., \tag{2.14b}$$

$$p = p_0 + \varepsilon p_1 + \varepsilon^2 p_2 + ..., \tag{2.14c}$$

$$\bar{S} = S\varepsilon^{-2}. \tag{2.14d}$$

The leading order in ε for the governing equations and boundary conditions are $O(1)$

$$u_{0x} + w_{0z} = 0, \tag{2.15a}$$

$$u_{0zz} + \sin\beta = 0, \tag{2.15b}$$

$$p_{0z} + \cos\beta = 0. \tag{2.15c}$$

At $z = 0$:

$$u_0 = 0. \tag{2.16}$$

At $z = h$:

$$u_{0z} = 0, \tag{2.17a}$$

$$-p_0 = \bar{S}^{-1} h_{xx}. \tag{2.17b}$$

Solving the above systems in $O(1)$, we obtain solutions for p_0, u_0 and w_0 as following:

$$p_0 = \cos\beta(h-z) - \bar{S}^{-1} h_{xx}, \tag{2.18a}$$

$$u_0 = \sin\beta(hz - \frac{1}{2}z^2), \tag{2.18b}$$

$$w_0 = -\sin\beta h_x \frac{1}{2}z^2. \tag{2.18c}$$

the governing system in $O(\varepsilon)$ is:

$$Re(u_{0t} + u_0 u_{0x} + w_0 u_{0z}) = -p_{0x} + u_{1zz}, \tag{2.19a}$$

$$p_{1z} = 0, \tag{2.19b}$$

$$u_{1x} + w_{1z} = 0. \tag{2.19c}$$

At $z = 0$:

$$u_1 = 0. \tag{2.20}$$

At $z = h$:

$$u_{1z} = 0, \tag{2.21a}$$

$$p_1 = \bar{p}_1(x,t). \tag{2.21b}$$

From the results of $O(1)$ terms, we have expression for each term in u_{1zz}:

$$p_{0x} = \cos\beta h_x - \bar{S}^{-1} h_{xxx}, \tag{2.22a}$$

$$u_{0x} = \sin\beta h_x z, \tag{2.22b}$$

$$u_{0t} = \sin\beta h_t z, \tag{2.22c}$$

$$u_{0z} = \sin\beta(h-z). \tag{2.22d}$$

Substitute the expressions in (2.19a)

$$u_{1zz} = \frac{1}{2} Re \sin^2\beta h h_x z^2 + Re \sin\beta h_t z + \cos\beta h_x - \bar{S}^{-1} h_{xxx}. \tag{2.23}$$

With the boundary conditions (2.20) and (2.21a) in $O(\varepsilon)$, we obtain solution for u_1

$$u_1 = \left(\cos\beta h_x - \bar{S}^{-1}h_{xxx}\right)\left(\frac{1}{2}z^2 - hz\right) + \frac{1}{6}Re\sin^2\beta h h_x\left(\frac{1}{4}z^4 - h^3 z\right) + \frac{1}{2}Re\sin\beta h_t\left(\frac{1}{3}z^3 - h^2 z\right). \tag{2.24}$$

Then solving (2.13) with $u = u_0 + \varepsilon u_1$ where algebraic expressions for u_0 and u_1 are known

$$\partial_t h + \partial_x \int_0^h (u_0 + \varepsilon u_1)\, dz = 0,$$

we have:

$$\int_0^h (u_0 + \varepsilon u_1)\, dz = \frac{1}{3}\sin\beta h^3 - \frac{1}{3}\varepsilon\left(\cos\beta h_x - \bar{S}^{-1}h_{xxx}\right)h^3 - \frac{5}{24}\varepsilon Re\sin\beta h_t h^4 - \frac{3}{40}\varepsilon Re\sin^2\beta h_x h^6$$

Finally we have the evolution equation for the film height:

$$h_t + G\sin\beta h^2 h_x - \frac{1}{3}\varepsilon[\cos\beta h_x h^3]_x + \frac{1}{3}\varepsilon[\bar{S}^{-1}h_{xxx}h^3]_x - \frac{3}{40}\varepsilon[Re\sin^2\beta h_x h^6]_x - \frac{5}{24}\varepsilon[Re\,(\sin\beta h_t)\,h^4]_x = 0. \tag{2.26}$$

In order to eliminate the h_t term in order ε, we take the leading order in the evolution equation for h

$$h_t + \sin\beta h^2 h_x = 0 \tag{2.27}$$

and substitute the h_t term in $O(\varepsilon)$, we get the final form of the evolution equation for the film thickness

$$h_t + \sin\beta h^2 h_x - \frac{1}{3}\varepsilon[\cos\beta h_x h^3]_x + \frac{1}{3}\varepsilon[\bar{S}^{-1}h_{xxx}h^3]_x + \frac{2}{15}\varepsilon[Re\sin^2\beta h_x h^6]_x = 0. \tag{2.28}$$

The dynamics of this simple film problem is important in continuing to more complicated problems. The dominating terms in this problem are only gravity, interfacial shear stress and capillary effect. While as we will be discussing in next chapter, the problem involves energy balance and concentration gradient. Understanding this problem will provide preliminary information on the behavior of the thin film.

Chapter 3

Binary Evaporating Films

In this chapter, we discuss the mathematical model and long wave theory for a binary thin fluid film down an inclined plane. The film is bounded by a heated solid surface with constant temperature from below and passive gas above. One fluid component is evaporating.

We propose a system of governing equations modelling the thin film. Follow the terminology from Chapter 2, first we require the conservation of mass of the system where no sink or source exists. [19]

$$\frac{\partial \rho}{\partial t^*} + \nabla \cdot (\rho \boldsymbol{u}^*) = 0, \tag{3.1}$$

where $\boldsymbol{u}^*$ is the liquid velocity and ρ is the density of the mixture.

Since the liquid is driven by gravity and falling down, we also require conservation of momentum and we use the Navier-Stokes equation [6, 20]

$$\rho \left(\frac{\partial \boldsymbol{u}^*}{\partial t^*} + \boldsymbol{u}^* \cdot \nabla \boldsymbol{u}^* \right) = -\nabla p^* + \mu \nabla^2 \boldsymbol{u}^* - \rho \boldsymbol{g}^* \tag{3.2}$$

where p^* is the pressure, μ is the dynamic viscosity and $\boldsymbol{g}^*$ is gravity.

The liquid mixture is heated by a solid surface from below, we anticipate energy transfer within the liquid, we then have the energy equation to model the temperature profile[6]

$$(\frac{\partial \theta^*}{\partial t^*} + \boldsymbol{u}^* \cdot \nabla \theta^*) = \kappa \nabla \theta^*, \tag{3.3}$$

where θ^* is the temperature, and κ is the thermal diffusivity.

Since the liquid is a mixture, we consider the concentration of the alcohol as the interest of the problem. C in this case is the mass fraction of alcohol and is balance by the mass flux within the liquid. [19]

$$\rho \frac{DC^*}{Dt^*} = -\nabla \cdot \boldsymbol{J}^*, \tag{3.4}$$

where $\boldsymbol{J}^*$ is the mass flux and it is expressed as [16]

$$\boldsymbol{J}^* = -\rho D(\nabla C^* + \frac{k_\theta}{\theta^*}\nabla\theta^*), \tag{3.5}$$

where k_θ is the thermal diffusion ratio.

Considering only 2-D problem, then we can express the above governing equations in scalar form below

$$u^*_{x^*} + w^*_{z^*} = 0, \tag{3.6a}$$

$$(u^*_{t^*} + u^* u^*_{x^*} + w^* u^*_{z^*}) = -\frac{1}{\rho}p^*_{x^*} + \nu(u^*_{x^*x^*} + u^*_{z^*z^*}) + g^*\sin\beta, \tag{3.6b}$$

$$(w^*_{t^*} + u^* w^*_{x^*} + w^* w^*_{z^*}) = -\frac{1}{\rho}p^*_{z^*} + \nu(w^*_{x^*x^*} + w^*_{z^*z^*}) - g^*\cos\beta, \tag{3.6c}$$

$$\theta^*_{t^*} + u^*\theta^*_{x^*} + w^*\theta^*_{z^*} = \kappa(\theta^*_{x^*x^*} + \theta^*_{z^*z^*}), \tag{3.6d}$$

$$\boldsymbol{J}^* = -\rho D(C_{x^*}\boldsymbol{i} + C_{z^*}\boldsymbol{k} + \frac{k_\theta}{\theta^*}\theta^*_{x^*}\boldsymbol{i} + \frac{k_\theta}{\theta^*}\theta^*_{z^*}\boldsymbol{k}), \tag{3.6e}$$

$$\rho(C^*_{t^*} + u^* C^*_{x^*} + w^* C_{z^*}) = -\rho D[C^*_{x^*x^*} + C^*_{z^*z^*} + \nabla\cdot(\frac{k_\theta}{\theta^*}\nabla\theta^*)]. \tag{3.6f}$$

Requiring no-slip and no flux at the solid surface, the boundary conditions at $z^* = 0$ is

$$u^* = 0, \qquad w^* = 0, \qquad \boldsymbol{J}^*\cdot\boldsymbol{k} = 0. \tag{3.7}$$

At $z^* = h(x^*, t^*)$, the boundary conditions include: jump mass balance, jump energy balance, normal and shear stress balance and mass flux: [12]

$$J^* = \rho^v(\bar{\boldsymbol{u}}^v - \bar{\boldsymbol{u}}^I)\cdot\hat{\boldsymbol{n}} = \rho(\bar{\boldsymbol{u}} - \bar{\boldsymbol{u}}^I)\cdot\hat{\boldsymbol{n}}, \tag{3.8a}$$

$$\begin{aligned} J^*\left(L + \frac{1}{2}[(\bar{\boldsymbol{u}}^v - \bar{\boldsymbol{u}}^I)\cdot\hat{\boldsymbol{n}}]^2 - \frac{1}{2}[(\bar{\boldsymbol{u}} - \bar{\boldsymbol{u}}^I)\cdot\hat{\boldsymbol{n}}]^2\right) + k\nabla\theta\cdot\hat{\boldsymbol{n}} - k^v\nabla\theta^v\cdot\hat{\boldsymbol{n}} \\ +2\mu(\bar{\boldsymbol{\tau}}\cdot\cdot\hat{\boldsymbol{n}})\cdot(\bar{\boldsymbol{u}} - \bar{\boldsymbol{u}}^I) - 2\mu^v(\bar{\boldsymbol{\tau}}^v\cdot\cdot\hat{\boldsymbol{n}})\cdot(\bar{\boldsymbol{u}}^v - \bar{\boldsymbol{u}}^I) = 0, \end{aligned} \tag{3.8b}$$

$$J^*(\bar{\boldsymbol{u}} - \bar{\boldsymbol{u}}^I)\cdot\hat{\boldsymbol{n}} - (\bar{\bar{T}} - \bar{\bar{T}}^v)\cdot\hat{\boldsymbol{n}}\cdot\hat{\boldsymbol{n}} = \nabla\sigma(\theta^*, C^*)\cdot\hat{\boldsymbol{n}}, \tag{3.8c}$$

$$J^*(\bar{\boldsymbol{u}} - \bar{\boldsymbol{u}}^I)\cdot\hat{\boldsymbol{t}} - (\bar{\bar{T}} - \bar{\bar{T}}^v)\cdot\hat{\boldsymbol{n}}\cdot\hat{\boldsymbol{t}} = -\nabla\sigma(\theta^*, C^*)\cdot\hat{\boldsymbol{t}}, \tag{3.8d}$$

$$\boldsymbol{J}^*\cdot\hat{\boldsymbol{n}} = \frac{\alpha\rho^v L}{T_s^{3/2}}\left(\frac{M_w}{2\pi R_g}\right)^{\frac{1}{2}}(T^I - T_s) + K^*_c C^*, \tag{3.8e}$$

where the superscript v and I represent vapor and interface respectively and the ones without represents the liquid, k is the thermal conductivity, $\bar{\bar{T}}$ is the stress tensor

$$\bar{\bar{T}} = -p\boldsymbol{I} + \mu(\nabla\vec{\boldsymbol{u}} + \nabla\vec{\boldsymbol{u}}^T), \tag{3.9}$$

$\hat{\boldsymbol{n}}$ and $\hat{\boldsymbol{t}}$ are normal and tangential vector to the free surface:

$$\hat{\boldsymbol{n}} = \frac{(-\varepsilon h_x, 1)}{(1+\varepsilon^2 h_x^2)^{1/2}}, \qquad \hat{\boldsymbol{t}} = \frac{(1, \varepsilon h_x)}{(1+\varepsilon^2 h_x^2)^{1/2}}. \tag{3.10}$$

In (3.8e) [21], α is the accommodation coefficient, R_g is the universal gas constant, M_w is the molecular weight and L is the latent heat. σ_0 is the surface tension and it is a function of temperature and concentration [18]

$$\sigma(\theta^*, C) = \sigma_0 - \gamma_\theta(\theta^* - \theta_R) - \gamma_c(C^* - C_R), \tag{3.11}$$

where σ_0 is the surface tension at reference temperature and concentration, γ_θ and γ_C are determined through experimental data.

To simplify the problem, we assume that the density, viscosity and thermal conductivity in the liquid are much greater than in the vapor except for (3.8a), then we take the limit in which all terms with a superscript v vanishes. In the jump energy balance, we also assume $\nabla T^v \cdot \boldsymbol{n}$, $\boldsymbol{\tau} \cdot \boldsymbol{n} \cdot \boldsymbol{n}$ and $\boldsymbol{\tau}^v \cdot \boldsymbol{n} \cdot \boldsymbol{n}$ are bounded and express velocities in terms of the mass flux and density from (3.8a), it becomes

$$J^* \left(L + \frac{1}{2}[\frac{J^*}{\rho^v}]^2 \right) = k \nabla\theta \cdot \hat{\boldsymbol{n}}, \tag{3.12}$$

and similarly the normal stress boundary condition is

$$-\frac{J^{*2}}{\rho^v} - \bar{\bar{T}} \cdot \boldsymbol{n} \cdot \boldsymbol{n} = \nabla\sigma(\theta^*, C^*) \cdot \hat{\boldsymbol{n}}, \tag{3.13}$$

and in the shear stress balance, assuming no-slip condition we get

$$\bar{\bar{T}} \cdot \hat{\boldsymbol{n}} \cdot \hat{\boldsymbol{t}} = \nabla\sigma(\theta^*, C^*) \cdot \hat{\boldsymbol{t}}, \tag{3.14}$$

We then non-dimensionalize the governing equations and boundary condition with the following scaling for long wave problem. Length is scaled on film mean thickness and the characteristic length, pressure is scaled on hydraulic pressure, velocity is scaled on gravity and kinematic viscosity and film height is scaled on the film mean thickness

$$z^* = d_0 z \qquad x^* = \frac{d_0}{\varepsilon} x \qquad p^* = \rho g^* d_0 p, \tag{3.15a}$$

$$u^* = \frac{g^* d_0^2}{\nu} u \qquad w^* = \varepsilon \frac{g^* d_0^2}{\nu} w \qquad t^* = \frac{\nu}{\varepsilon g^* d_0} t, \tag{3.15b}$$

$$h^* = d_0 h \qquad \theta = \frac{\theta^* - \theta_R}{\theta_H - \theta_R} \qquad J^* = \frac{k\Delta\theta}{d_0 L} J. \tag{3.15c}$$

where θ_H is the constant temperature at $z = 0$, θ_R is the reference temperature.

We assume the existence of ambient alcohol concentration near the interface, so depending on the situation, the deviation concentration may be negative in cases where the ambient alcohol exists in large amount and condensation occurs.

$$C = \frac{C^* - C_{atm}}{C_{am}} \tag{3.16}$$

where C_{atm} is the ambient concentration.

Then we define ε on the based on the characteristic length scale. $\varepsilon = \frac{d_0}{L}$ where L is determined by $L^2 = \frac{d_0^2}{\nu^2 \rho}$ which results a characteristic length of 3.4 cm and given d_0 of 0.01 cm, ε is of order 10^{-2}.

After applying the scaling to the governing system, we achieve at the following

$$u_x + w_z = 0, \tag{3.17a}$$

$$\varepsilon Re(u_t + uu_x + wu_z) = -\varepsilon p_x + \varepsilon^2 u_{xx} + u_{zz} + \sin\beta, \tag{3.17b}$$

$$\varepsilon^2 Re(w_t + uw_x + ww_z) = -p_z + \varepsilon^3 w_{xx} + \varepsilon w_{zz} - \cos\beta, \tag{3.17c}$$

$$\varepsilon RePr(\theta_t + u\theta_x + w\theta_z) = \varepsilon^2 \theta_{xx} + \theta_{zz}, \tag{3.17d}$$

$$\boldsymbol{J} = -ReSc(\varepsilon C_x \boldsymbol{i} + C_z \boldsymbol{k} + \varepsilon \frac{k_\theta}{\theta} \theta_x \boldsymbol{i} + \frac{k_\theta}{\theta} \theta_z \boldsymbol{k}), \tag{3.17e}$$

$$\varepsilon ReSc(C_t + uC_x + wC_z) = \varepsilon^2 C_{xx} + C_{zz} + \varepsilon^2 [\frac{k_\theta}{\theta} \theta_x]_x + [\frac{k_\theta}{\theta} \theta_z]_z. \tag{3.17f}$$

where

$$Re = \frac{g^* d_0^3}{\nu^2}, \qquad Sc = \frac{\nu}{D} \qquad Pe = ReSc \tag{3.18}$$

The scaled boundary conditions at the heated solid surface $z = 0$, no slip, no mass flux across and constant temperature

$$u = 0 \tag{3.19a}$$

$$w = 0 \tag{3.19b}$$

$$\theta = 1 \tag{3.19c}$$

$$C_z + \frac{k_\theta}{\theta} \theta_z = 0 \tag{3.19d}$$

At free surface $z = h(x,t)$, we assume constant ambient temperature and pressure, and including mass flux due to evaporation [13] [19]

$$EJ = \frac{\varepsilon w - \varepsilon h_t - \varepsilon u h_x}{(1 + \varepsilon^2 h_x^2)^{1/2}} \tag{3.20a}$$

$$J + E^2 B^{-2} Re \mathscr{L}^{-1} J^3 = \frac{\varepsilon^2 \theta_x h_x - \theta_z}{(1+\varepsilon^2 h_x^2)^{1/2}} \tag{3.20b}$$

$$-E^2 B^{-1} Re^{-1} J^2 + p - \frac{2[\varepsilon u_x(\varepsilon^2 h_x^2 - 1) - \varepsilon h_x(\varepsilon^2 w_x + u_z)]}{1+\varepsilon^2 h_x^2} = -S(1 - M_\theta \theta)\frac{\varepsilon^2 h_{xx}}{(1+\varepsilon^2 h_x^2)^{3/2}} \tag{3.20c}$$

$$(u_z + \varepsilon^2 w_x)(1-\varepsilon^2 h_x^2) - 4\varepsilon^2 u_x h_x = -\varepsilon\{M_\theta(\theta_x + \theta_z h_x) + M_c(C_x + C_z h_x)\}(1+\varepsilon^2 h_x^2)^{1/2} \tag{3.20d}$$

$$J = K_\theta \theta + K_c C \tag{3.20e}$$

where M_θ and M_c are thermal and solutal Marangoni number, $\mathscr{L}$ is the measure of latent heat and all parameters are defined as:

$$B = \frac{\rho^v}{\rho} \qquad E = \frac{k\Delta\theta\nu}{\rho g^* d_0^3 L}, \tag{3.21a}$$

$$\mathscr{L} = \frac{L}{g^* d_0} \qquad M_\theta = \frac{\gamma_\theta \Delta\theta d_0}{2\rho\nu^2}, \tag{3.21b}$$

$$M_c = \frac{\gamma_c \Delta\theta d_0}{2\rho\nu^2} \qquad S = \varepsilon^2 \frac{\sigma_0 d_0}{\nu^2 \rho} = O(1), \tag{3.21c}$$

$$K_\theta = \left(\frac{d_0 \alpha \rho^v L^2}{k\Delta\theta T_s^{3/2}}\right)\left(\frac{M_w}{2\pi R_g}\right)^{1/2}. \tag{3.21d}$$

In order to understand the scaled parameters, we calculate the magnitude of each scaled parameter, the typical values of the independent and constant parameters are: [12]

Table 3.1: Constant Parameters

	Parameter	Value	Unit
Pressure	p	1.01×10^6	g/cm.s^2
Initial film thickness	d_0	0.002	cm
Temperature difference	ΔT	10	K
Gravity	g	980	cm/s^2
Aspect ratio	ε	10^{-2}	

Table 3.2: Liquid parameter

	Parameter	Water	Ethanol	Unit
Reference Temperature	T_s	373	352	K
Liquid Density	ρ	0.96	0.79	g/cm^3
vapor Density	ρ^v	6×10^{-4}	1.6×10^{-3}	g/cm ^{3}
Kinematic Viscosity	ν	3×10^{-3}	5×10^{-3}	cm^2/s
vapor Kinematic Viscosity	ν^v	0.21	0.62	cm^2/s
Thermal Conductivity	k	6.8×10^4	1.7×10^4	erg/cm·K·s
vapor Thermal Conductivity	k_v	2.4×10^3	1.3×10^3	erg/cm·K·s
Thermal Diffusivity	κ	1.7×10^{-3}	8.8×10^{-4}	cm^2/s
vapor Thermal Diffusivity	κ^v	0.2	0.07	cm^2/s
Latent Heat	L	2.3×10^3	8.8×10^2	J/g
Molecular Weight	M_w	18	46	g/mole
	γ_θ	0.18	0.9	dynes/cm·K

Table 3.3: Dimensionless parameters

Parameter	Water	Ethanol
Re	2.94	0.314
Pe	7.1×10^2	1.27×10^2
B	6.25×10^{-4}	2.03×10^{-3}
E	3.49×10^{-3}	1.56×10^{-2}
$\mathscr{L}$	7.82×10^2	4.49×10^1
M	3.13×10^2	4.56×10^4

In order to seek the solution of the governing system, we expand dependent variables in powers of ε:

$$u = u_0 + \varepsilon u_1 + \varepsilon^2 u_2 + ..., \tag{3.22a}$$

$$w = w_0 + \varepsilon w_1 + \varepsilon^2 w_2 + ..., \tag{3.22b}$$

$$p = p_0 + \varepsilon p_1 + \varepsilon^2 p_2 + ..., \tag{3.22c}$$

$$\theta = \theta_0 + \varepsilon \theta_1 + \varepsilon^2 \theta_2 + ..., \tag{3.22d}$$

$$J = J_0 + \varepsilon J_1 + \varepsilon^2 J_2 + ..., \tag{3.22e}$$

$$C = C_0 + \varepsilon C_1 + \varepsilon^2 C_2 + ... \tag{3.22f}$$

Asymptotic expansion of the temperature fraction term becomes

$$\frac{\theta_z}{\theta} = \frac{\theta_{0z} + \varepsilon\theta_{1z} + \varepsilon^2\theta_{2z}}{\theta_0 + \varepsilon\theta_1 + \varepsilon^2\theta_2} = \frac{\theta_{0z}}{\theta_0} + \varepsilon\left(\frac{\theta_{1z}}{\theta_0} - \frac{\theta_{0z}}{\theta_0}\left[\frac{\theta_1}{\theta_0}\right]\right) \tag{3.23}$$

We start by assuming that Reynolds number is negligible and we require $Sc \neq 0$ so we introduce Peclet number:

$$Pe = Re\ Sc = \frac{d_0 U}{D} \tag{3.24}$$

and we let Pe be finite. J_0, K_θ and K_c are of order ε. We first solve for the evolution equation of the film. The system of order $O(1)$ is

$$0 = u_{0zz} + \sin\beta, \tag{3.25a}$$

$$0 = -p_{0z} - \cos\beta, \tag{3.25b}$$

$$0 = \theta_{0zz}, \tag{3.25c}$$

$$0 = [C_{0z} + \frac{k_\theta}{\theta_0}\theta_{0z}]_z. \tag{3.25d}$$

The boundary conditions of $O(1)$ at $z = 0$ are:

$$u_0 = 0, \tag{3.26a}$$

$$w_0 = 0, \tag{3.26b}$$

$$\theta_0 = 1, \tag{3.26c}$$

$$C_{0z} + \frac{k_\theta}{\theta_0}\theta_{0z} = 0. \tag{3.26d}$$

At $z = h(x,t)$

$$EJ_0 = w_0 - h_t - u_0 h_x, \tag{3.27a}$$

$$0 = \theta_{0z}, \tag{3.27b}$$

$$p_0 = -Sh_{xx}, \tag{3.27c}$$

$$u_{0z} = 0, \tag{3.27d}$$

$$J_0 = K_\theta \theta_0 + K_c C_0. \tag{3.27e}$$

Then we achieve at the solutions for independent variables:

$$u_0 = \sin\beta\,(hz - \frac{1}{2}z^2), \tag{3.28a}$$

$$w_0 = -\frac{1}{2}\sin\beta\, h_x z^2, \tag{3.28b}$$

$$p_0 = \cos\beta\,(h - z) - Sh_{xx}, \tag{3.28c}$$

$$\theta_0 = 1, \tag{3.28d}$$

$$C_0 = \bar{c}_0, \tag{3.28e}$$

$$J_0 = K_\theta + K_c \bar{c}_0. \tag{3.28f}$$

At $O(\varepsilon)$, the governing system and boundary conditions are as follows

$$0 = -p_{0x} + u_{1zz}, \tag{3.29a}$$

$$0 = \theta_{1zz}, \tag{3.29b}$$

$$Pe(C_{0t} + u_0 C_{0x}) = \{C_{1z} + k_\theta \theta_{1z}\}_z. \tag{3.29c}$$

At $z = 0$;

$$\theta_1 = 0, \tag{3.30a}$$

$$C_{1z} + k_\theta \theta_{1z} = 0. \tag{3.30b}$$

At $z = h(x,t)$

$$J_1 = -\theta_{1z}, \tag{3.31a}$$

$$u_{1z} = -M_c \bar{c}_{0x}, \tag{3.31b}$$

$$\frac{J_1}{Pe} = -(C_{1z} + k_\theta \theta_{1z}), \tag{3.31c}$$

$$J_1 = K_\theta \theta_1 + K_c C_1. \tag{3.31d}$$

Solving for u_1 and θ_1 term, we get:

$$\theta_1 = -J_1 z, \tag{3.32}$$

$$u_1 = p_{0x}(\frac{1}{2}z^2 - hz) - M_c \bar{c}_{0x} z \tag{3.33}$$

where

$$p_{0x} = \cos\beta h_x - Sh_{xxx}. \tag{3.34}$$

Recall the evolution equation of the film thickness in simple film. Follow the same derivation but with an additional flux term, we integrate the continuity equation over $z = 0$ to $z = h(x,t)$ and achieve the evolution equation for the film thickness.

$$h_t + EJ + \partial_x \int_0^h u dz = 0, \tag{3.35}$$

$$h_t + EJ_0 + \partial_x \int_0^h (u_0 + \varepsilon u_1) dz = 0, \tag{3.36}$$

$$\begin{aligned} \int_0^h u_1 dz = \int_0^h \left(p_{0x}(\frac{1}{2}z^2 - hz) - M_c \bar{c}_{0x} z \right) dz &= -\frac{1}{3} p_{0x} h^3 - \frac{1}{2} M_c \bar{c}_{0x} h^2 \\ &= \frac{1}{3} Sh_{xxx} h^3 - \frac{1}{3} \cos\beta h_x h^3 - \frac{1}{2} M_c \bar{c}_{0x} h^2. \end{aligned} \tag{3.37}$$

Then we have the evolution equation up to $O(\varepsilon^2)$

$$h_t + \sin\beta h_x h^2 + E\left(K_\theta + K_c\bar{c}_0\right) + \varepsilon\partial_x\left(\frac{1}{3}Sh_{xxx}h^3 - \frac{1}{3}\cos\beta h_x h^3 - \frac{1}{2}M_c\bar{c}_{0x}h^2\right) = O(\varepsilon^2). \quad (3.38)$$

Then we need to solve for the evolution equation of concentration field. By integrating (3.29c) once over $z = 0$ to $z = h(x,t)$ and applying boundary conditions (3.30b) and (3.31c), we get:

$$\int_0^h (\bar{c}_{0t} + u_0\bar{c}_{0x})dz = \frac{1}{Pe}[C_{1z} + k_\theta\theta_{1z}]\Big|_0^h, \quad (3.39)$$

$$\bar{c}_{0t} + \frac{1}{3}\sin\beta h^2\bar{c}_{0x} = -\frac{1}{Pe^2}\left(\frac{K_\theta + K_c\bar{c}_0}{h}\right). \quad (3.40)$$

Equation (3.38) and (3.40) are the coupled evolution equations we will be studying in the next chapter.

Chapter 4

Results

4.1 Spatially Independent Solution

We seek the analytical space independent solutions to (3.38) and (3.40) and assume $K_\theta = 0$. The system of equations becomes

$$h_t + EK_c\bar{c}_0 = 0, \tag{4.1a}$$

$$\bar{c}_{0t} + \frac{K_c}{Pe^2}\left(\frac{\bar{c}_0}{h}\right) = 0. \tag{4.1b}$$

This system is easier to solve than the original system because there are fewer variables and terms of order ε was omitted, and leaving this simplified system.

As $t \to \infty$, $\bar{c}_0$ approaches 0, while h approaches a final height h_f. In order to find the algebraic expression for h_f, we first differentiate eq.(4.1a) with respect to time once and substitute expression for $\bar{c}_0$ and $\bar{c}_{0t}$

$$h_{tt} = -\frac{K_c}{Pe^2}\left(\frac{h_t}{h}\right). \tag{4.2}$$

Then integrate both sides over $t = 0$ to $t = \tau$, to get:

$$h_t\big|_{t=\tau} - h_t\big|_{t=0} = \frac{K_c}{Pe^2}[\ln(h)|_{t=\tau} - \ln(h)\big|_{t=0}]. \tag{4.3}$$

Given the initial conditions $h(0)$ and $\bar{c}_0(0)$ for the film and concentration, we have the expression for the film thickness at steady state as

$$h_t = \frac{K_c}{Pe^2}\ln(h) - \frac{K_c}{Pe^2}\ln(h(0)) - EK_c\bar{c}_0(0) \tag{4.4}$$

4.2 Linear Stability Theory

Now we consider the linear stability of the exact solution to (3.38) and (3.40). Assume a perturbation on the base state of the solution

$$\begin{pmatrix} h \\ c_0 \end{pmatrix} = \begin{pmatrix} h_f \\ 0 \end{pmatrix} + \delta \begin{pmatrix} \hat{H} \\ \hat{C} \end{pmatrix} e^{i\alpha x + \sigma t} \tag{4.5}$$

where δ is an infinitesimally small amplitude, α is the wavenumber, and σ is the growth rate of the disturbance.

Then applying the form (4.5) to the system of (3.38) and (3.40) and only keep the terms which are independent of δ, we have the following system

$$\begin{pmatrix} \sigma + i\sin\beta\,\alpha h_f^2 + \varepsilon(\frac{1}{3}S\alpha^4 h_f^3 + \frac{1}{3}\cos\beta\,\alpha^2 h_f^3) & EK_c + \varepsilon(\frac{1}{2}M_c\alpha^2 h_f^2) \\ 0 & \sigma + i\frac{1}{3}\sin\beta\,\alpha h_f^2 + \frac{K_c}{Pe^2 h_f} \end{pmatrix} \begin{pmatrix} \hat{H} \\ \hat{C} \end{pmatrix} = \begin{pmatrix} 0 \\ 0 \end{pmatrix}. \tag{4.6}$$

We find the solution to the growth rate σ by letting the determinant of the above 2-by-2 matrix to be zero

$$\sigma_h = -i\sin\beta\,\alpha h_f^2 - \varepsilon(\frac{1}{3}S\alpha^4 h_f^3 + \frac{1}{3}\cos\beta\,\alpha^2 h_f^3), \tag{4.7}$$

$$\sigma_c = -i\frac{1}{3}\sin\beta\,\alpha h_f^2 - \frac{K_c}{Pe^2 h_f}. \tag{4.8}$$

Then the phase speeds are

$$\mathrm{Im}\left(\frac{\sigma_h}{\alpha}\right) = -\sin\beta h_f^2, \tag{4.9}$$

$$\mathrm{Im}\left(\frac{\sigma_c}{\alpha}\right) = -\frac{1}{3}\sin\beta h_f^2. \tag{4.10}$$

And the growth rates are

$$\mathrm{Re}(\sigma_h) = -\varepsilon(\frac{1}{3}S\alpha^4 h_f^3 + \frac{1}{3}\cos\beta\,\alpha^2 h_f^3), \tag{4.11}$$

$$\mathrm{Re}(\sigma_c) = -\frac{K_c}{Pe^2 h_f}. \tag{4.12}$$

There is no instability in the film as S, β, and h_f are all positive, the growth rates of the film and concentration are always negative. Infinitesimal small perturbations in the film and concentration field eventually decay as the thin film continues flowing down. The base state solution is stable.

We include the inertia term in the film evolution equation. Similarly, we apply the form (4.5) to the system and achieve at the expression of the matrix

$$\begin{pmatrix} \sigma + i\sin\beta\alpha h_f^2 + \varepsilon(\frac{1}{3}S\alpha^4 h_f^3 + \frac{1}{3}\cos\beta\alpha^2 h_f^3 - \frac{2}{15}Re\sin^2\beta\alpha^2 h_f^6) & EK_c + \varepsilon(\frac{1}{2}M_c\alpha^2 h_f^2) \\ 0 & \sigma + i\frac{1}{3}\sin\beta\alpha h_f^2 + \frac{K_c}{Pe^2 h_f} \end{pmatrix}. \tag{4.13}$$

The growth rate of the film is:

$$Re(\sigma_h) = -\varepsilon(\frac{1}{3}S\alpha^4 h_f^3 + \frac{1}{3}\cos\beta\alpha^2 h_f^3 - \frac{2}{15}Re\sin^2\beta\alpha^2 h_f^6). \tag{4.14}$$

The inertia term is destabilizing the film and this is consistent with previous works. For simplicity, we assume the final film height is $h_f = 1$, for $\beta = \pi/4$, $Re = 5$ and $S = 1$, we have the growth rate as a function of wavenumber:

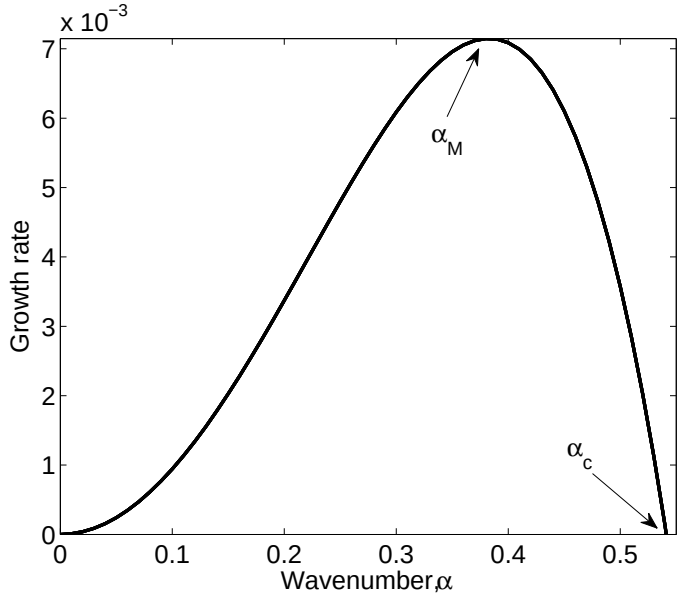

Figure 4.1: Grwoth rate vs wavenumber, parameter values are: $\beta = \pi/4$, $Re = 5$ and $S = 1$

We introduce a cutoff wavenumber α_c which is wavenumber that separates the stable and unstable modes of the film and α_M which is the wavenumber at which the growth rate of the film is the largest:

$$\alpha_c = \sqrt{\frac{1}{S}\left(\frac{2}{5}Re\sin^2(\beta) - \cos(\beta)\right)} \tag{4.15}$$

$$\alpha_M = \sqrt{\frac{1}{S}\left(\frac{1}{5}Re\sin^2(\beta) - \frac{1}{2}\cos(\beta)\right)} \tag{4.16}$$

We are interested in the situations where the film has a positive growth rate (unstable) and how the film evolves as it grows in time. Obviously, the film is most unstable when $\beta = \pi/2$. Then we have this most dangerous wavenumber which we will use for later simulations:

$$\alpha_M = \sqrt{\frac{Re}{5S}} \tag{4.17}$$

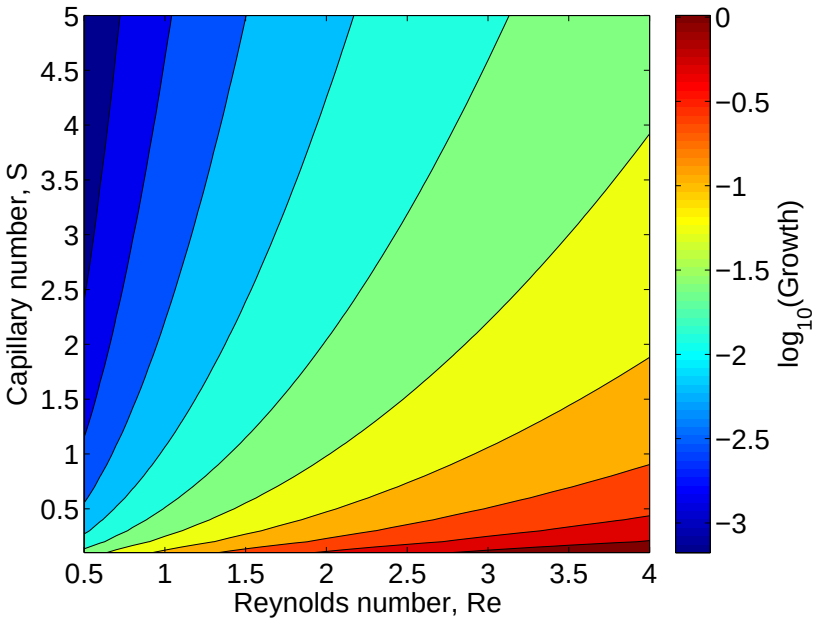

Figure 4.2: Relations between maximum growth rate and Re and S when $\beta = \pi/2$

Then we investigate how the parameters affect the maximum growth rate. From Figure 4.2, we can see that as the Reynolds number increases, the growth rate increases while as the Capillary number increases, the growth rate decreases. The linear stability analysis suggests that the film is stable as long as inclination angle is small or the wavenumber is sufficiently large.

4.3 Matlab Script Validation

There are numerous ways to solve the system, the methods we use are forward Euler and Crank-Nicolson. We compare the results solved by both methods in order to validate the script through checking the degree of accuracy of each solution. Crank-Nicolson method has error of order Δt^2 whereas Forward Euler method has error of order Δt. In order to validate Matlab script, we first solve the system found in space independent solution with both methods and then solve eq.(4.18) which is a first order differential equation of h only with a given value of $h(0)$ and $\bar{c}_0(0)$. Then we compare the solutions by these two methods with the "exact" results from the single equation.

$$h_t = -\frac{K_c}{Pe^2}\ln(h(0)) - EK_c\bar{c}_0(0) - \frac{K_c}{Pe^2}\ln(h) \tag{4.18}$$

No analytical solution can be found for eq.(4.18), we will solve it numerically with Matlab ode solver. Since we will use this result as the "exact" solution for comparison, in order to obtain the solution which is very close to the exact solution, we ensure that the tolerance for the solution is very small. The error shown below is calculated as $E = \|h_f - h_a\|$ where h_f is the final solution and h_a is the "exact" solution.

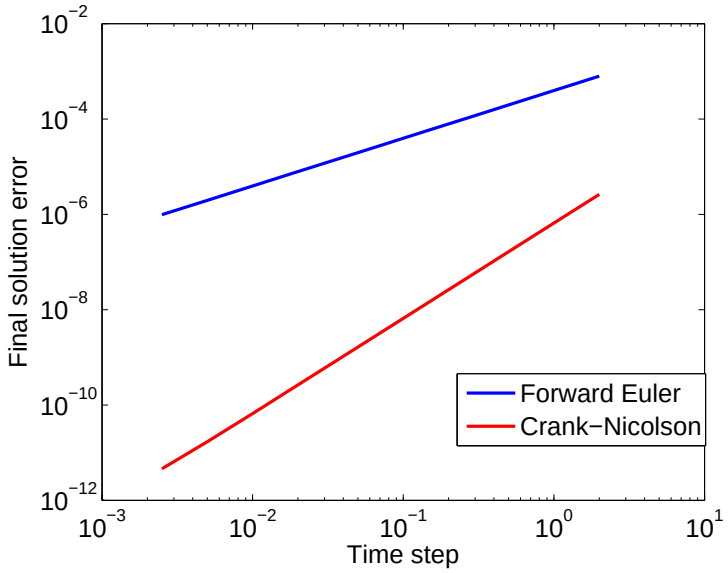

Figure 4.3: Log-log plot of the solution error at different time step. Slope for forward Euler is 1 and that for Crank-Nicolson is 2. Simulation Runtime is 30 seconds

Then we investigate only the film equation with initially concentration being zero. Many previous works have studied this and we will briefly show the result to further validate our code.

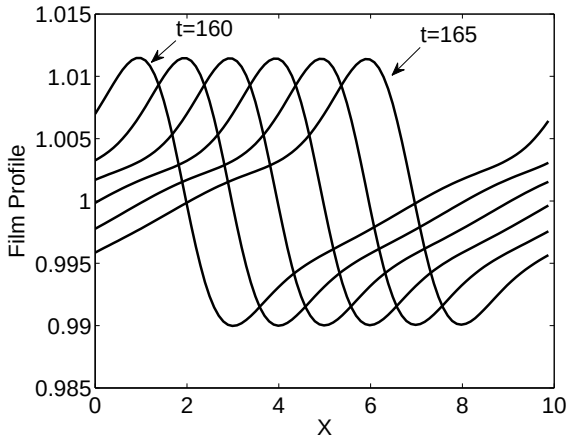

Figure 4.4: Film shape at $t = 160s$ to $t = 165s$. $\Delta t = 0.1s$. Parameter values: $\beta = \pi/2$, $Re = 1$, $S = 0.5$, $k = 0.63$, $\varepsilon = 0.01$.

As the film of single component evolves over time, Figure 4.4 showed the travelling wave from $t = 160s$ to $165s$. The pattern changes slowly with time.

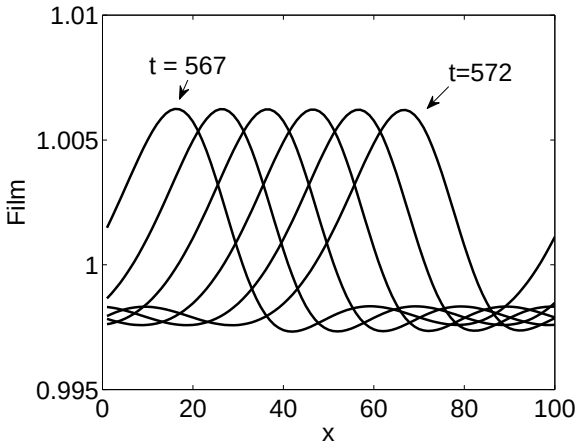

Figure 4.5: Film shape from $t = 567s$ to $t = 572s$. $\Delta t = 0.1s$. Parameter values: $\beta = \pi/2$, $Re = 1$, $S = 0.5$, $k = 0.63$, $\varepsilon = 0.01$.

4.4 Film Shape Transition

We start with a stable film with no perturbation. Initial conditions are $h(x,0) = 1$ and $C(x,0) = 0.1 + 0.01\cos(kx)$. For a initially flat film, the variation in the concentration field will result in the wave pattern. Figure. 4.6 is the evolution of film and concentration over space and time.

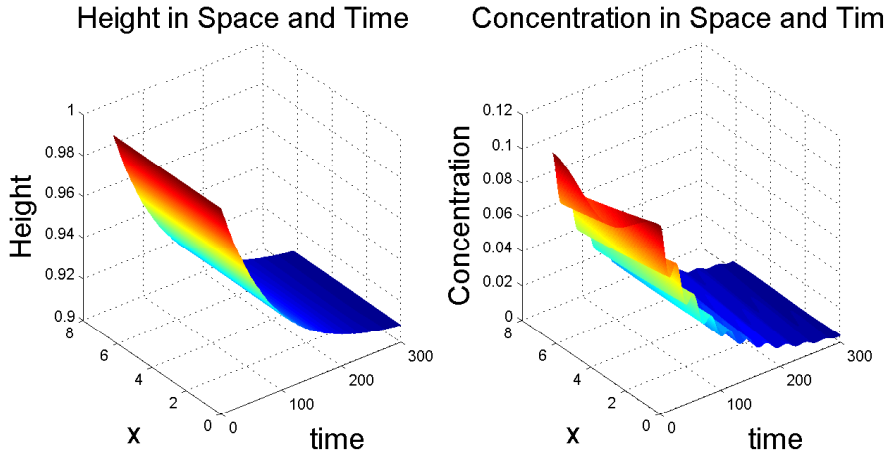

Figure 4.6: Film and concentration evolve over time. $\beta = \pi/4$, $Pe = 1$, $M = Re = 0$, $E = 1$, $K_c = 0.01$ and $S = 1$.

The film is flat at the beginning, as the concentration field travels, a wave pattern starts to form in the film. From figure. 4.7, at around $t = 14$, $t = 27$, and $t = 40$, when the peak of concentration field coincides with the peak of the film, the peak of the film will shift by half of the wave period.

The formation of the wave pattern in the film is primarily due to the condensation and evaporation disequilibrium. Since concentration has a cosine profile about zero, the film will have an evaporation (condensation) profile of a sine curve and this will lead to the wave pattern in the film. As we can see at $t = 0$, the peak of the film starts from half period and this is where the concentration is the lowest at the beginning. Because the film and concentration travel at different speeds, the peaks of the film and concentration will eventually meet each other and then the evaporation or condensation effects will again pull the peak of the film towards the position where the concentration is lowest.

The amplitude of the film also varies with time. It increases when the film and concentration profile curve differ by half period. The minimum amplitude appears every 13.4 in this case (the film will have local minimum amplitude at each 13.4 interval). Figure 4.8 shows the profiles of film and concentration at $t = 12.4$ and $t = 13.4$. In about 1 second, the difference in the positions of film and concentration profile changed from 0 to $\pi/4$.

In order to further investigate this phenomena, we will first test how each parameter influences the dynamic. We will use the following initial condition for the following results:

$$h(x,0) = 1 \qquad C(x,0) = 0.01\cos(kx) \tag{4.19}$$

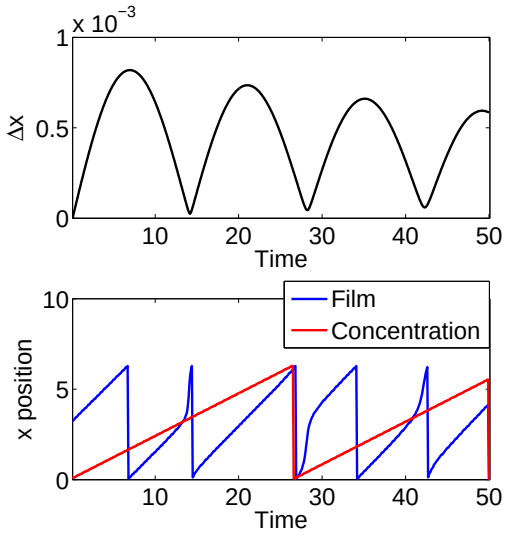

Figure 4.7: Top plot shows the magnitude of the film amplitude vs. time and bottom shows the positions of the peaks in film and concentration profiles vs. time. Parameter values are: $\beta = \pi/4$, $Pe = 1$, $M = Re = 0$, $E = 1$, $K_c = 0.01$ and $S = 1$

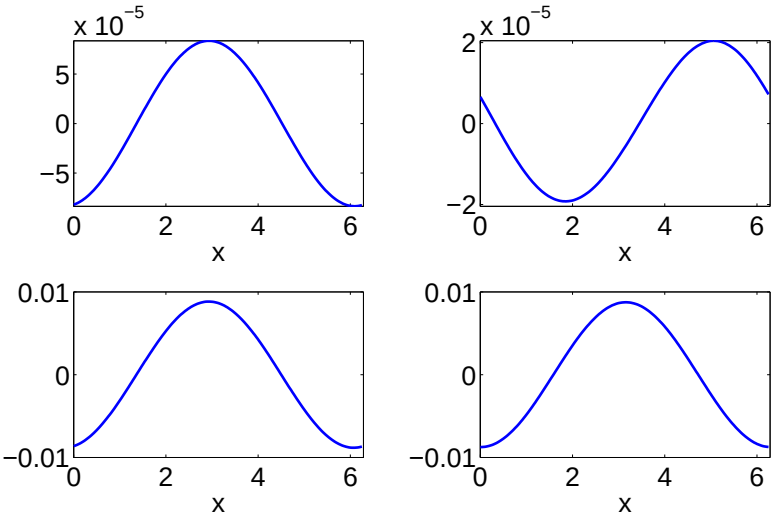

Figure 4.8: Left is when $t = 12.4$ and right $t = 13.4$. Parameter values are: $S = 0.1$, $Pe = 1$, $\beta = \pi/4$, $M = Re = 0$, $E = 1$, $K_c = 0.01$.

Concentration field with mean of 0 is used, so that the overall film height will not change due to either evaporation or condensation. As we defined the concentration to be a relative concentration, so it can be either positive (evaporating) or negative (condensing). We will increase and decrease each parameter by tenth and investigate how the dynamics change.

As captioned in figure.4.7, the following plots represent the same information. Top plots are

the magnitude of the film amplitude, middle plots are the positions of the peaks in film and concentration profiles and bottom plots are the amplitude in concentration field (See Appendix. C for all plots).

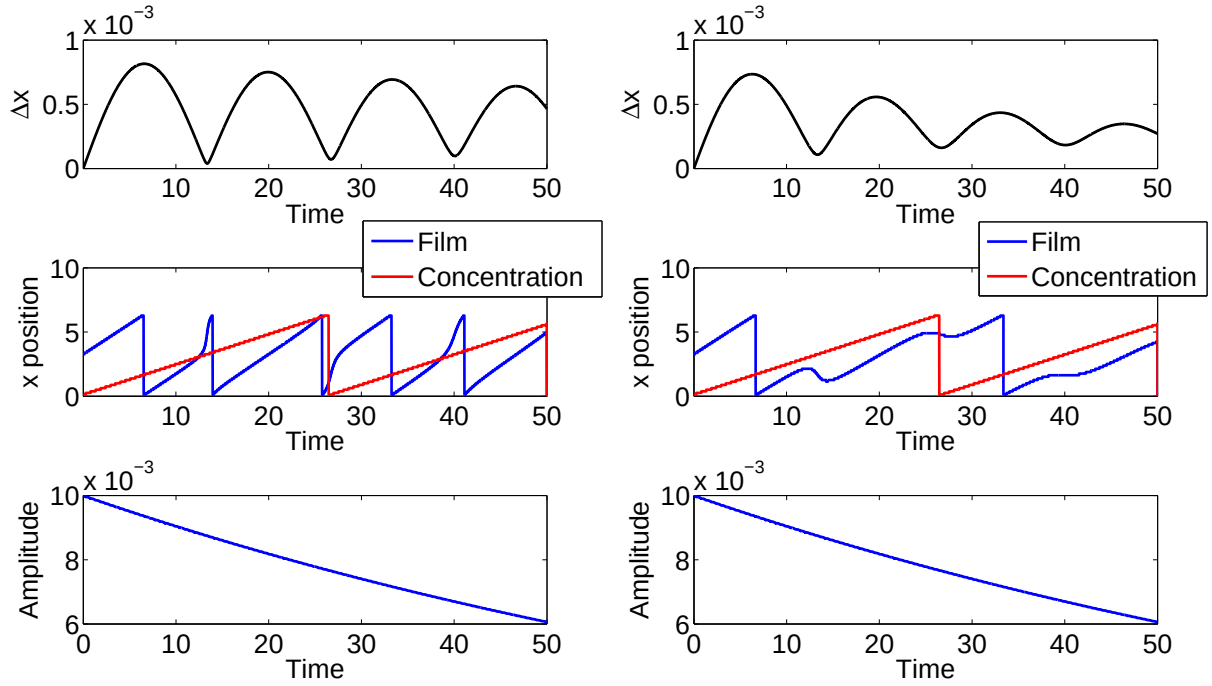

Figure 4.9: Left plots are when $S = 0.1$ and right $S = 10$. Other Parameter values are: $\beta = \pi/4$, $Pe = 1$, $M = Re = 0$, $E = 1$, $K_c = 0.01$.

There are two main types of variations that will occur when varying the values of each parameter. We will consider the result of $\beta = \pi/4, S = 1, Pe = 1, E = 1$, and $K_c = 0.01$ as our standard in the following comparison. Increase S, Pe, E and decreasing K_c will result in the film perturbation shifts backward instead of shifting forward when the peaks of concentration and film coincide. Decreasing Pe, Decreasing E and increasing K_c will reduce the peak shift phenomena. Increasing β not only changes the speed of the film and concentration, and also decreases the amplitude of the wave resulted from the concentration. Decreasing S will only slight speed up the film stabilization and slow down the speed of the peak shift. In the following, we will discuss three cases in details. In order to achieve so, the film profile will be plot at consecutive time during the shift along with the effects from each term in the film evolution equation.

4.4.1 Shift forward

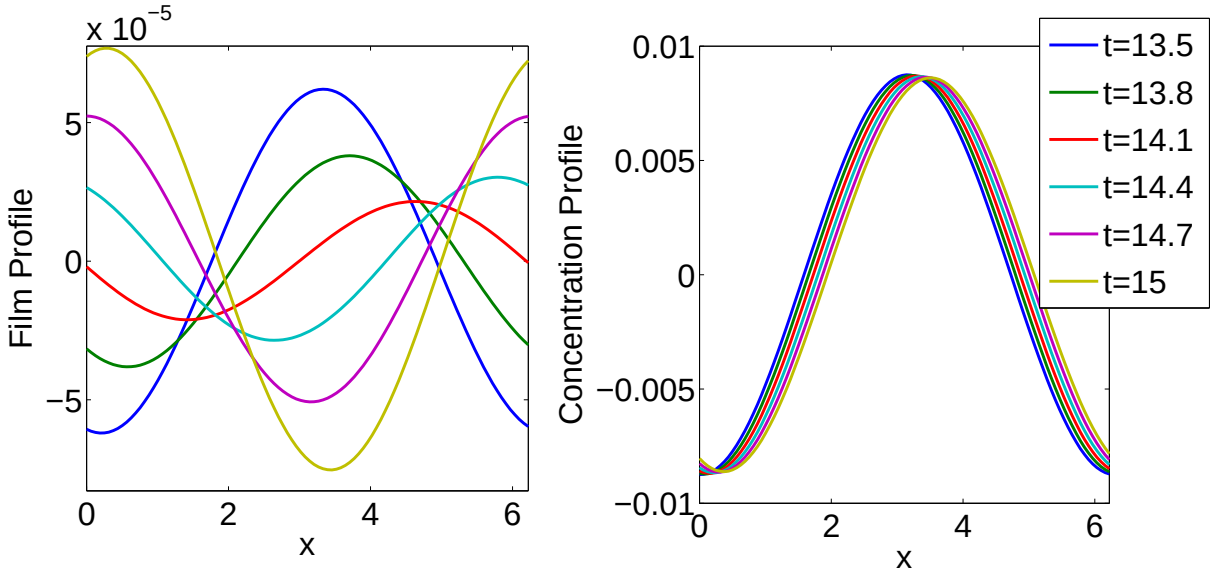

Figure 4.10: Film and concentration profile at consecutive times during the sharp transition. Parameter values are: $S = 0.1$, $Pe = 1$, $\beta = \pi/4$, $M = Re = 0$, $E = 1$, $K_c = 0.01$.

Ideally, the film should travel three time as fast as the concentration field. As the concentration travels one period in space, the film will have travelled about 3 periods. Below is the single component stable film travelling without any concentration effects.

$$h_t + \sin(\beta)h^2 h_x + \cdots = 0 \qquad\qquad c_t + \frac{1}{3}\sin(\beta)h^2 c_x + \cdots = 0 \tag{4.20}$$

However, with perturbation of the concentration, the actual travelling speed of the film is only twice as much as the concentration (when the speed is nearly constant). The film speed for the simple falling film is about 0.707 s^{-1}, whereas in the case of peak shifting forward, the film speed is only 0.47 s^{-1}. So the concentration effect (evaporation and condensation) generally will slow down the travelling speed of the film. Figure. 4.11 shows the effects from each term in the film evolution equation. The evaporation term are of order 10^{-4} while all the rest terms are much smaller. So in this case, it is purely the evaporation effect that is causing the quick peak shift of the film.

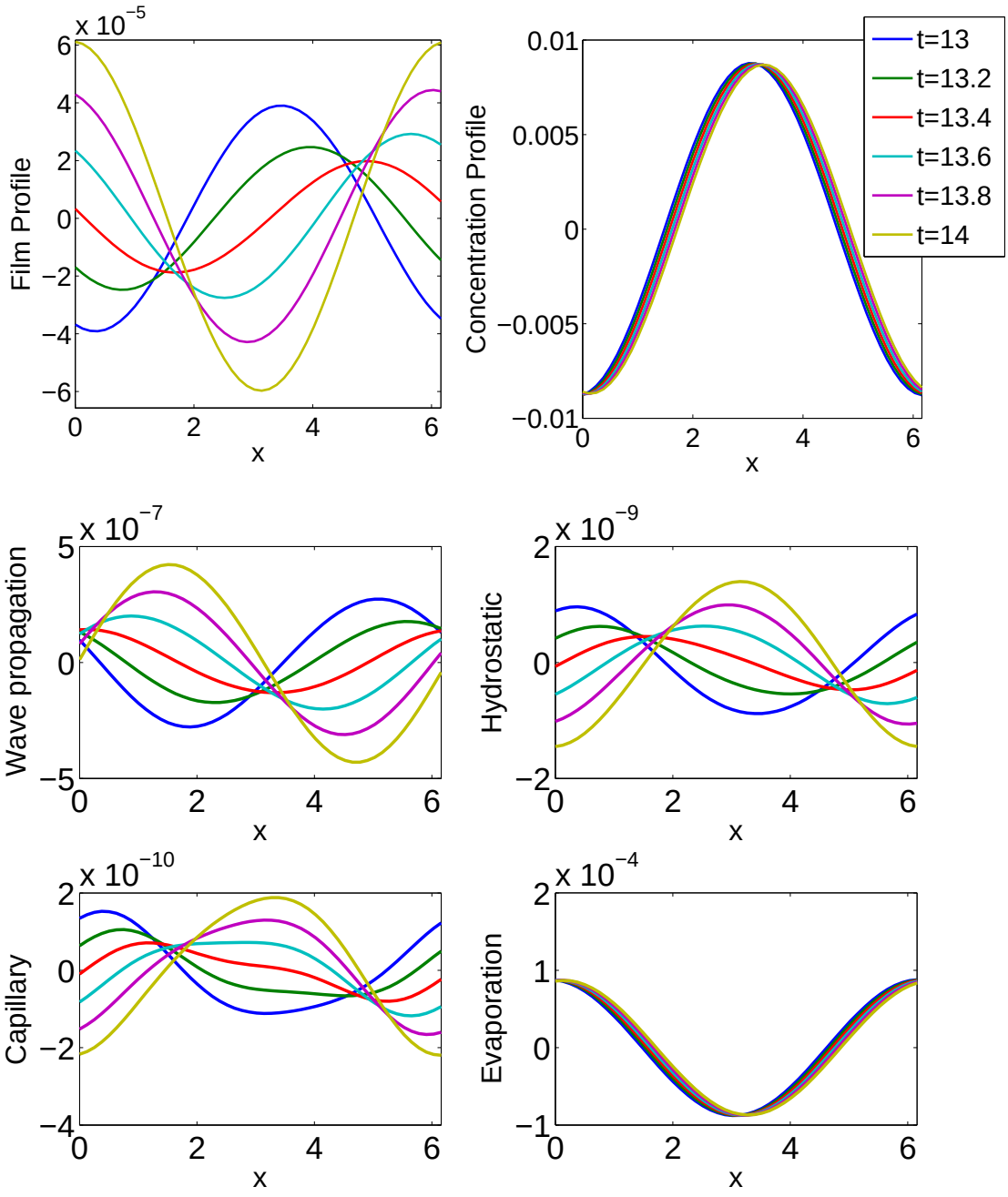

Figure 4.11: The magnitude of each effect at different time. Parameter values are: $S = 0.1$, $Pe = 1$, $\beta = \pi/4$, $M = Re = 0$, $E = 1$, $K_c = 0.01$.

4.4.2 Shift Backward

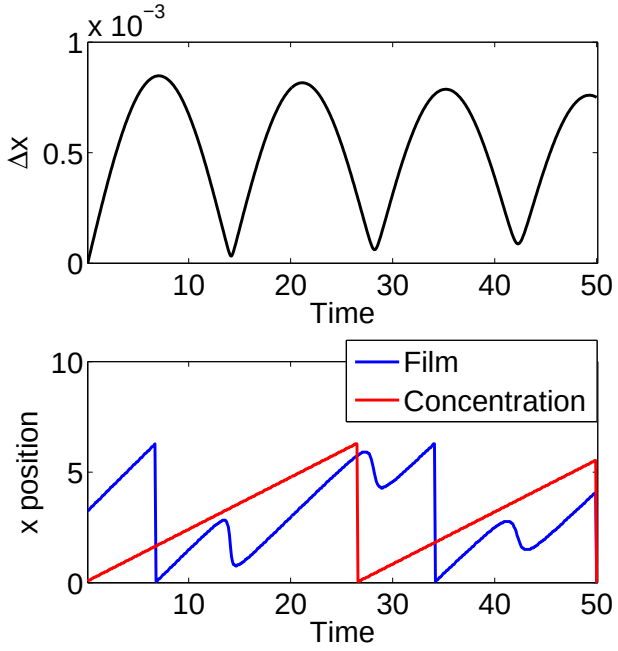

Figure 4.12: Parameter values are: $S = 1$, $Pe = 10$, $\beta = \pi/4$, $M = Re = 0$, $E = 1$, $K_c = 0.01$.

This is a case where the dynamics of the film is different from what we discovered in previous section. The film travels backward when the peaks of concentration and film meet. Selecting the first peak transition as our interest of study. Limit the time to $t = [12.5; 14]$ with time increment of 0.3. Figure. 4.14 shows the magnitude of the effects from each term.

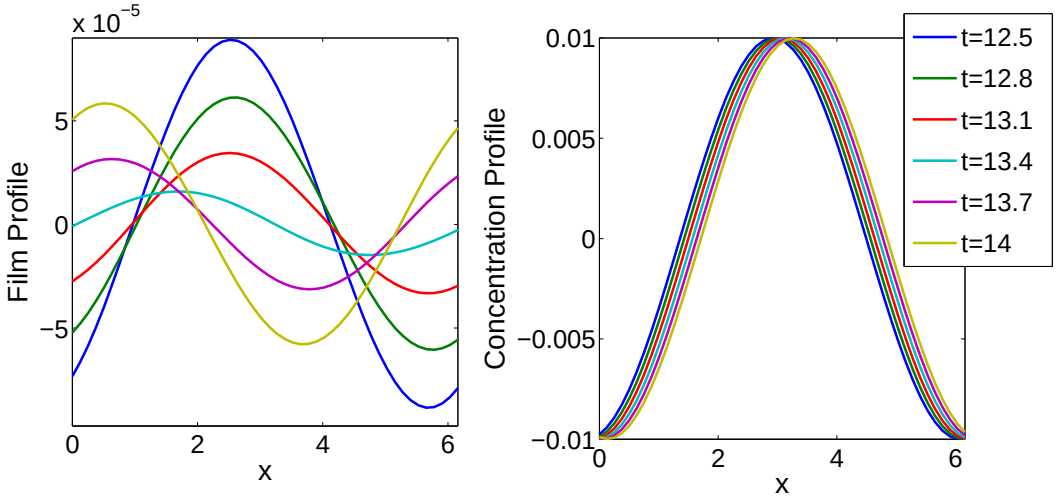

Figure 4.13: Parameter values are: $S = 1$, $Pe = 10$, $\beta = \pi/4$, $M = Re = 0$, $E = 1$, $K_c = 0.01$.

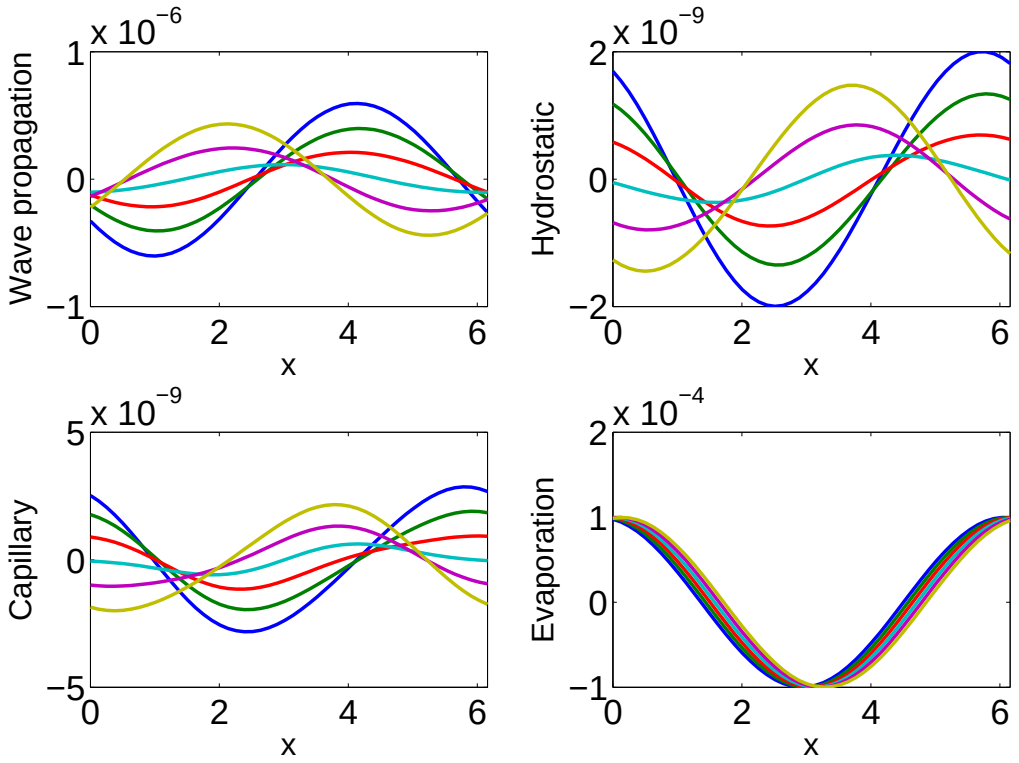

Figure 4.14: The magnitude of each effect at different time. Parameter values are: $S = 1$, $Pe = 1$, $\beta = \pi/4$, $M = Re = 0$, $E = 10$, $K_c = 0.01$.

4.4.3 Peak Jump

This phenomena is different from the previous two cases because there is no shift pattern and the film profile is not a cosine curve anymore. Two local peaks will form in the film. And the change of the global peak position depends on the variation of each local peak. So we will see a instantaneous peak position change. To gain better resolution for the analysis, we increase the number of spatial step from 100 to 200 and decrease time step from 0.1s to 0.01s. We will set $C(x,0) = 0.05\cos(kx)$ and other parameters as $S = 1$, $Pe = 1$, $\beta = \pi/4$, $M = Re = 0$, $E = 10$, $K_c = 0.01$.

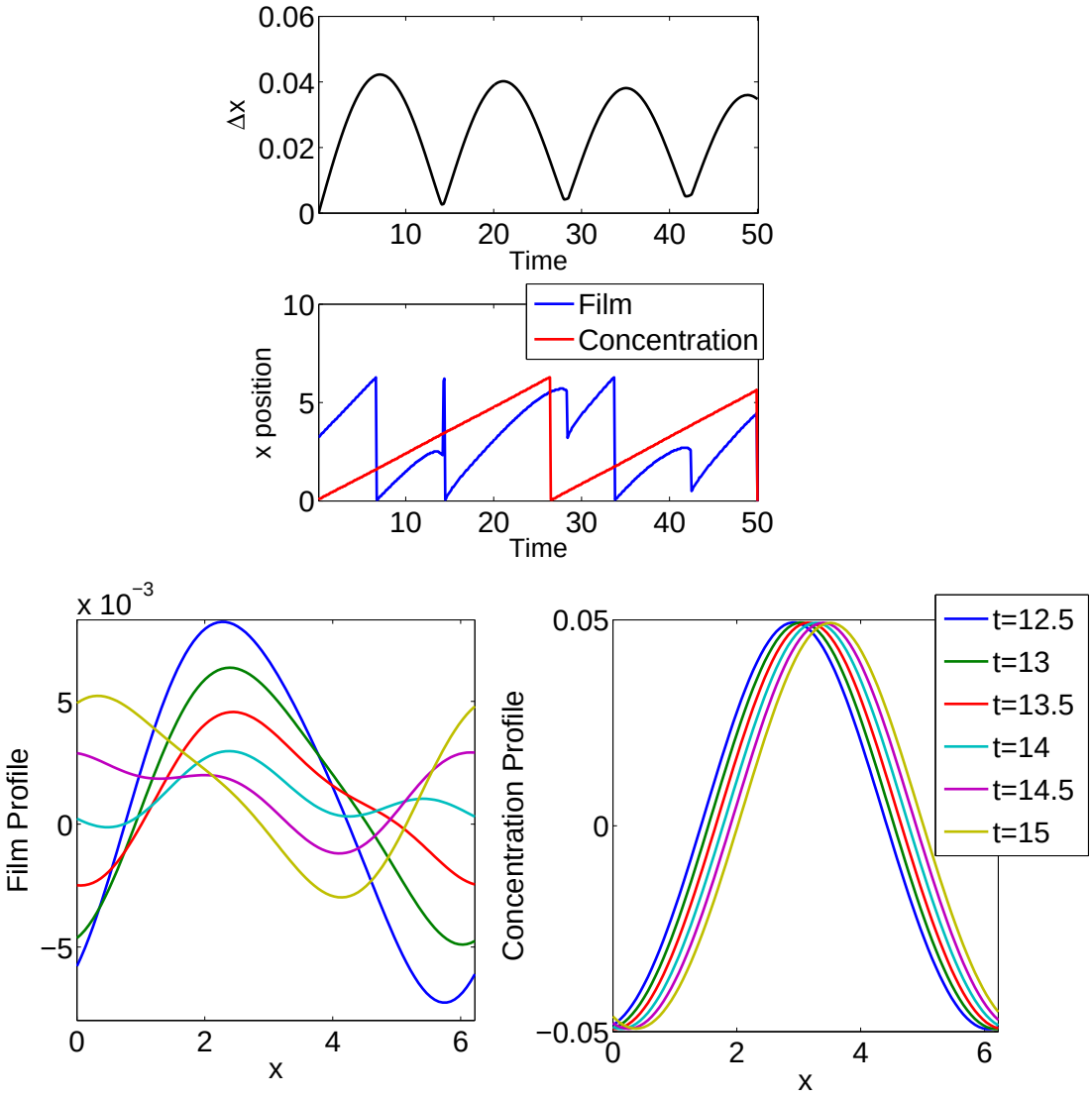

Figure 4.15: Parameter values are: $S = 1$, $Pe = 1$, $\beta = \pi/4$, $M = Re = 0$, $E = 10$, $K_c = 0.01$.

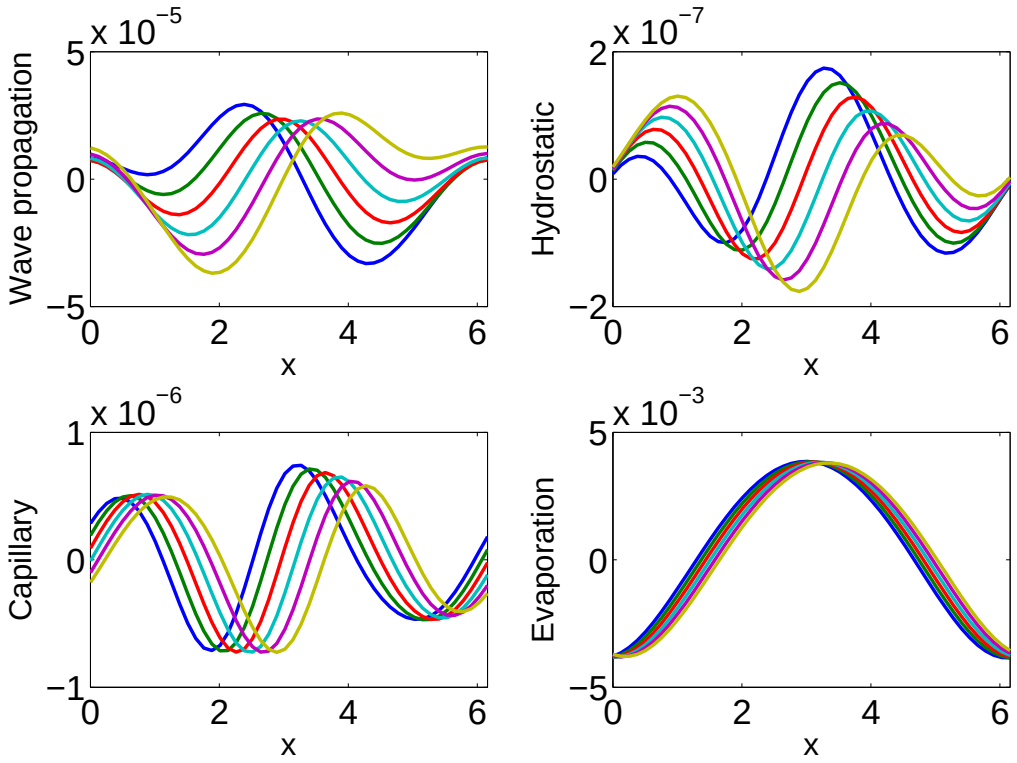

Figure 4.16: Parameter values are: $S = 1$, $Pe = 1$, $\beta = \pi/4$, $M = Re = 0$, $E = 10$, $K_c = 0.01$.

Chapter 5

Conclusion

In this project, we have studied the evaporation(condensing) effects on a two-dimensional falling film of a two component fluid with one being volatile. We started with the Benney's problem and expanded upon the work by Joo *etal*. The film is modelled based on long wave theory and perturbation theory is applied. Nondimensionalization was utilized in order to reduce the number of parameters and have better understanding of the dominating effects. After obtaining the evolution equations for both the film and concentration, we applied linear stability theory and developed several numerical methods to solve for the film and concentration profiles by assuming the periodic boundary condition. We then focused on the different dynamics we have discovered during numerical simulation and studied the effects of evaporation and condensation on the film profile.

With an initially flat film and a variation in the concentration, although eventually the film is stable, we still have discovered some interesting phenomena that for different sets of parameter values, the film will perform quite different dynamics. Due to the different speeds of the film and concentration field, the profiles of film and concentration will have interactions as they travel. Based on the difference between the minimal amplitude when the film and concentration profiles overlap and the concentration profile, the wave in the film will either shift forward, backward or have a jump.

The amplitude in the film is completely due to the evaporation or condensation (variation in the concentration field). Increasing the initial amplitude on the film or increasing Marangoni number will increase the amplitude, but it will not change the dynamics of film (See Appendix D). As a result, we will not focus on how high the film goes with different concentration and Marangoni number. We will discuss in details on explaining the previous findings.

First we need to understand why the film amplitude varies when it travels. As we have discussed, the amplitude in the film is caused by the concentration disequilibrium that the evaporation or condensation rate are different at different locations of the film. As the film travels, a wave pattern on the film will appear and ideally it will be the inverse of the wave pattern in the concentration field. But because of the different travelling speeds of film and concentration, the film profile on the film will gradually approaches and overlaps with that in the concentration. Take

the case where the peak shift forward as an example, the concentration starts with a cosine curve whereas the resultant film profile will be a sine curve, so their peaks are distant by half period ($\pi/2$). As the film and concentration travel, the amplitude in the film increases (we will call this increasing phase) until the distance between the two peaks is $\pi/4$, and this is when the amplitude starts to decrease (we will call this decreasing phase). When the two peaks meet, peak on the film will shift forward by half a period and repeats the pattern over and over.

As we vary different parameters, we are changing either the film or the concentration or both of them. Although the concentration depends on the film height, the variation on the film is so small that it will not have any significant effect. So if one parameter appears only in the film equation, it will affect much more on the film than on concentration.

From the previous plots, it is obvious that during the transition, the concentration effect dominates the dynamics. However, as we vary different parameters, the film has shown quite different dynamics. For example, $S = 1$, the film will shift forward as the peak of the film and concentration fields meet, however as we increase S, the film will shift backwards. The capillary effect doesn not have any influence on the film during the transition, but it does before the transition. The capillary effect will tend to keep the wave motion, thus reduce the amount of amplitude loss during the decreasing phase as the film profile approaches the concentration profile.

As for the shift forward case, both the film and concentration during the shift are relative small, and we will call this as the cooperative case. When we increase the film amplitude before the shift or we increase the concentration during shift, the film will shift backwards and we will have a competing case. Either the film is large enough to overcome the concentration effect, resulting the film to shift backward, or the concentration is too large that the film speed is not fast enough to past through the ”concentration effect”. Then as for the cases where the peak of the film jumps (occurrence of two local peaks), the film amplitude is high enough to not be completely influenced by concentration, meanwhile the concentration is high enough to form another peak in the film. So the phenomena we discovered are the interaction between the film amplitude before the transition and the concentration effect.

To continue with further investigation, a clear relation on how the interaction is between the minimal film height and concentration effect could be established and further studied. In this report, we studies mainly the dynamics with small concentration, the same analysis could be done with higher concentration. An initial perturbation could be given to the film along with high concentration, we would expect that the dyanmics would be very interesting. Local temperature could also be introduced to the analysis.

Appendix A

Numerical Methods

For a non-linear PDE, sometimes it's very difficult or even impossible to obtain analytical solutions. In order to study the behavior of the PDE, discretization allows us to numerically solve the PDE. In this section, the subscript represents space and superscript represents time.

A.1 Central Difference

For spatial derivatives, second order central differencing method is used. This is a basic approach to obtain the derivative terms. Central differencing results in an error of second order in x which is enough for our problem, as long as the Δx is small. For first order derivative:

$$\left.\frac{\partial h}{\partial x}\right|_{x_i} = \frac{h_{i+1} - h_{i-1}}{2\Delta x} + O(\Delta x^2) \tag{A.1}$$

Second order derivative:

$$\left.\frac{\partial^2 h}{\partial x^2}\right|_{x_i} = \frac{h_{i+1} - 2h_i + h_{i-1}}{\Delta x^2} + O(\Delta x^2) \tag{A.2}$$

Third order derivative:

$$\left.\frac{\partial^3 h}{\partial x^3}\right|_{x_i} = \frac{h_{i+2} - 2h_{i+1} + 2h_{i-1} - h_{i-2}}{2\Delta x^3} + O(\Delta x^2) \tag{A.3}$$

Fourth order derivative:

$$\left.\frac{\partial^4 h}{\partial x^4}\right|_{x_i} = \frac{h_{i+2} - 4h_{i+1} + 6h_i - 4h_{i-1} + h_{i-2}}{\Delta x^4} + O(\Delta x^2) \tag{A.4}$$

In the simulation, derivative matrice were constructed for computational purposes.

$$h_x^i = D_1 h^i \tag{A.5}$$

where h^i is the vector of the height at time i, h_x^i is the vector of the first derivative at time i and D is a tridiagonal square matrix with as follows:

$$D_1 = \frac{1}{2\Delta x}\begin{bmatrix} 0 & 1 & 0 & 0 & \cdots & 0 & -1 \\ -1 & 0 & 1 & 0 & \cdots & 0 & 0 \\ 0 & -1 & 0 & 1 & \cdots & 0 & 0 \\ 0 & 0 & -1 & 0 & \cdots & 0 & 0 \\ \vdots & \vdots & \vdots & \vdots & \ddots & \vdots & \vdots \\ 0 & 0 & 0 & 0 & \cdots & 0 & 1 \\ 1 & 0 & 0 & 0 & \cdots & -1 & 0 \end{bmatrix} \tag{A.6}$$

Note there are entries in the upper right and low left of the matrix. Periodic boundary condition is used in the simulation, so this will give a smooth derivative at the boundaries. D_2, D_3 and D_4 matrices share the same pattern:

$$D_2 = \frac{1}{\Delta x^2}\begin{bmatrix} -2 & 1 & 0 & 0 & \cdots & 0 & 1 \\ 1 & -2 & 1 & 0 & \cdots & 0 & 0 \\ 0 & 1 & -2 & 1 & \cdots & 0 & 0 \\ 0 & 0 & 1 & -2 & \cdots & 0 & 0 \\ \vdots & \vdots & \vdots & \vdots & \ddots & \vdots & \vdots \\ 0 & 0 & 0 & 0 & \cdots & -2 & 1 \\ 1 & 0 & 0 & 0 & \cdots & 1 & -2 \end{bmatrix} \tag{A.7}$$

A.2 Forward Euler Method

We will use this generalized evolution equation for illustration in each methods below:

$$h_t + A(h)h_x + \varepsilon \left[B(h)h_x + S(h)h_{xxx} + C(h)c_x\right]_x = 0, \tag{A.8}$$

and

$$h_t = F(x,t,h,h_x,h_{xx},h_{xxx},h_{xxxx}) \tag{A.9}$$

Starting with Taylor expansion of h:

$$h^{t+\Delta t} = h^t + \Delta t \, \frac{\partial h^t}{\partial t} + \Delta t^2 \, \frac{\partial^2 h^t}{\partial t^2} + O(\Delta t^3) \tag{A.10}$$

Omitting the term with order Δt^2 and higher, we achieve at the forward Euler method which will solves the equation explicitly.

$$h^{t+\Delta t} = h^t + \Delta t \; F^t \tag{A.11}$$

Local trncation error resulted from euler method is of order Δt^2, whereas the global truncation error is of order Δt. In order to achieve adequate accuracy, small time step is required when using euler method.

A.3 Backward Euler Method

Backward Euler method is similar to the normal (forward) Euler method, but backward Euler is an implicit method. Instead of solving the derivative in time with the current state, backward Euler uses the future state:

$$h^{t+\Delta t} = h^t + \Delta t \; F^{t+\Delta t} \tag{A.12}$$

In order to solve the implicit equation, we use NewtonRaphson method.

$$h^{t+\Delta t} = h^t - \Delta t \frac{F^{t+\Delta t}}{F'^{t+\Delta t}} \tag{A.13}$$

For easy computation, we will construct Jacobian matrix to solve the equation.

$$h^{t+\Delta t} = h^t + (I + \Delta t J) \, F^{t+\Delta t} \tag{A.14}$$

where J is the jacobian matrix of F in terms of h_x. Jacobian matrix for $A(h) = \sin(\beta) h_x h^2$ is:

$$J_A = \begin{bmatrix} h_1^2 & 0 & 0 & \cdots & 0 \\ & h_2^2 & 0 & \cdots & 0 \\ 0 & 0 & h_3^2 & \cdots & 0 \\ \vdots & \vdots & \vdots & \ddots & \vdots \\ 0 & 0 & 0 & \cdots & h_n^2 \end{bmatrix} D_1 + \begin{bmatrix} h_1 h_{1x} & 0 & 0 & \cdots & 0 \\ & h_2 h_{2x} & 0 & \cdots & 0 \\ 0 & 0 & h_3 h_{3x} & \cdots & 0 \\ \vdots & \vdots & \vdots & \ddots & \vdots \\ 0 & 0 & 0 & \cdots & h_n h_{nx} \end{bmatrix} \tag{A.15}$$

A.4 Crank-Nicolson Method

Crank Nicolson method averages the results from the current and future time and result in a better estimation of the future state $O(\Delta t^2)$.

$$\frac{h^{n+1}-h^n}{\Delta t} = \frac{1}{2}\left(f^{n+1}+f^n\right) \tag{A.16}$$

We linearize the system with the following estimation. As the time step is small, H and C should be very small.

$$h^{n+1} = h^n + H \tag{A.17}$$

$$\bar{c}_0^{n+1} = \bar{c}_0^n + C \tag{A.18}$$

So we linearize the system with the above estimation:

$$\begin{aligned} h_t + \sin\beta h_x h^2 + EK_c\bar{c}_0 + \varepsilon\partial_x\left(\frac{1}{3}Sh_{xxx}h^3 - \frac{1}{3}\cos\beta h_x h^3 - \frac{1}{2}M_c\bar{c}_{0x}h^2\right. \\ \left. + \frac{2}{15}Re\sin^2(\beta)h_x h^6\right) = 0, \\ \bar{c}_{0t} + \frac{1}{3}\sin\beta h^2\bar{c}_{0x} + \frac{K_c}{EPe^2}\left(\frac{\bar{c}_0}{h}\right) = 0. \end{aligned}$$

Each term is linearized as the following:

$$\sin(\beta)h_x h^2 = \sin(\beta)\left(h_x^n (h^n)^2 + \frac{1}{2}Hh^n h_x^n + \frac{1}{2}H_x (h^n)^2\right) \tag{A.19a}$$

$$EK_c \bar{c}_0 = EK_c (c^n + C) \tag{A.19b}$$

$$\frac{1}{3}Sh_{xxxx}h^3 = \frac{1}{3}S\left(h_{xxxx}^n (h^n)^3 + \frac{1}{2}H_{xxxx}(h^n)^3 + \frac{3}{2}H(h^n)^2 h_{xxxx}^n\right) \tag{A.19c}$$

$$Sh_{xxx}h_x h^2 = S\left(h_{xxx}h_x^n (h^n)^2 + \frac{1}{2}H_{xxx}h_x^n (h^n)^2 + \frac{1}{2}H_x h_{xxx}(h^n)^2 + Hh_{xxx}h_x^n h^n\right) \tag{A.19d}$$

$$\cos(\beta)h_x^2 h^2 = \cos(\beta)\left((h_x^n)^2 (h^n)^2 + H_x h_x^n (h^n)^2 + H(h_x^n)^2 h^n\right) \tag{A.19e}$$

$$\frac{1}{3}\cos(\beta)h_{xx}h^3 = \frac{1}{3}\cos(\beta)\left(h_{xx}^n (h^n)^3 + \frac{1}{2}H_{xx}h^3 + \frac{3}{2}Hh_{xx}^n (h^n)^2\right) \tag{A.19f}$$

$$\frac{1}{2}M_c \bar{c}_{0xx}h^2 = \frac{1}{2}M_c\left(\bar{c}_{0xx}^n (h^n)^2 + \frac{1}{2}C_{xx}(h^n)^2 + C\bar{c}_{0xx}^n h^n\right) \tag{A.19g}$$

$$M_c \bar{c}_{0xx}h_x h = M_c\left(\bar{c}_{0xx}^n h_x^n h^n + \frac{1}{2}C_{xx}h_x^n h^n + \frac{1}{2}H_x \bar{c}_{0xx}^n h^n + \frac{1}{2}H\bar{c}_{0xx}^n h_x^n\right) \tag{A.19h}$$

$$\frac{4}{5}Re\sin^2(\beta)h_x^2 h^5 = \frac{4}{5}Re\sin^2(\beta)\left((h_x^n)^2 (h^n)^5 + H_x h_x^n (h^n)^5 + \frac{5}{2}H(h_x^n)^2 (h^n)^4\right) \tag{A.19i}$$

$$\frac{2}{15}Re\sin^2(\beta)h_x h^6 = \frac{2}{15}Re\sin^2(\beta)\left(h_x^n (h^n)^6 + \frac{1}{2}H_x (h^n)^6 + 3Hh_x^n (h^n)^5\right) \tag{A.19j}$$

$$\frac{1}{3}\sin\beta h^2 \bar{c}_{0x} = \frac{1}{3}\sin(\beta)\left((h^n)^2 \bar{c}_{0x}^n + \frac{1}{2}C(h^n)^2 + Hh^n \bar{c}_{0x}\right) \tag{A.19k}$$

$$\frac{K_c}{EPe^2}\frac{\bar{c}_0}{h} = \frac{K_c}{EPe^2}\left(\frac{\bar{c}_0^n}{h^n} + \frac{C}{h^n} - \frac{H\bar{c}_0^n}{(h^n)^2}\right) \tag{A.19l}$$

Then combine the film and concentration vector as:

$$\vec{v} = \begin{bmatrix} H \\ C \end{bmatrix} \tag{A.20}$$

And substitute all the linearized terms into the original system, we obtain a linear system of $\vec{v}$. Then we can solve it with matrix operation and get the result of the difference between the state at future time and current state.

$$\begin{bmatrix} L_{11} & L_{12} \\ L_{21} & L_{22} \end{bmatrix}\begin{bmatrix} H \\ C \end{bmatrix} = \begin{bmatrix} R_1 \\ R_2 \end{bmatrix} \tag{A.21}$$

where L_{11} and L_{12} are the matrices corresponds to the film equation whereas the L_{21} and L_{22} to the concentration equation. R_1 and R_2 are the vectors of the current state.

Appendix B

Matlab code

B.1 Second Order Crank-Nicolson Solver

```
function [film conc A B Ch Ev debug] = accucranknicolson()

% this file solves the time dependent solution to the film equation
% h_t +E*K_c*C + A(h)*h_x+ epsilon*(B(h)*h_x)+C(h)*h_xxx + D(h) *c_x)_x=0
% h(t,x,derivative)
% 2pi periodic
global E K_c M_c epsilon beta Re S k Nx xend dx dt tend tsize x H C Pe

debug=0;A=zeros(size(H));B=A;Ch=A;Ev=A;

%%% Derivative Matrices %%%
%%%% first derivative
Dc1 = diag(ones(Nx-1,1),1)+diag(-ones(Nx-1,1),-1);%%%central
Dc1(1,end) = -1; Dc1(end,1) = 1;
Dc1 = 1/2/dx*Dc1;

%%%% second derivative
Dc2 = diag(ones(Nx-1,1),1) + diag(-2*ones(Nx,1))+diag(ones(Nx-1,1),-1);
Dc2(1,end) = 1; Dc2(end,1) = 1;
Dc2 = 1/dx^2*Dc2;

%%%% third derivatve
Dc3 = diag(ones(Nx-2,1),2) - diag(2*ones(Nx-1,1),1)...
    +diag(2*ones(Nx-1,1),-1)-diag(ones(Nx-2,1),-2);
Dc3(1,end-1:end)=[-1 2]; Dc3(2,end) = -1;
Dc3(end-1:end,1)=[1 -2]; Dc3(end,2) = 1;
Dc3 = 1/2/dx^3*Dc3;

%%%% fourth derivative
Dc4 = diag(ones(Nx-2,1),2)+diag(-4*ones(Nx-1,1),1)...
```

```
    +diag(6*ones(Nx,1)) +diag(-4*ones(Nx-1,1),-1)...
    +diag(ones(Nx-2,1),-2);
Dc4(1,end-1:end) = [1 -4]; Dc4(2,end)=1;
Dc4(end-1:end,1) = [1 -4]; Dc4(end,2)=1;
Dc4 = 1/dx^4*Dc4;

%% solve with crank nicolson
for i = 1:tsize
    hh = H(:,i);
    cc = C(:,i);
    HC = [hh;cc];

    M11 = 1/dt*diag(ones(Nx,1),0)...
        +1/2*sin(beta)*(diag(hh.^2)*Dc1+diag(hh)*diag(Dc1*hh))...%advection
        +epsilon*1/6*S*(diag(hh.^3)*Dc4+3*diag(hh.^2)*diag(Dc4*hh))...%cap1
        +epsilon*1/2*S*(diag(hh.^2)*diag(Dc1*hh)*Dc3...     %cap2
                        +diag(hh.^2)*diag(Dc3*hh)*Dc1...
                        +2*diag(hh)*diag(Dc1*hh)*diag(Dc3*hh))...
        -epsilon*1/6*cos(beta)*(diag(hh.^3)*Dc2 ...
                        + 3*diag(Dc2*hh)*diag(hh.^2))...hydro1
        -epsilon*1/2*cos(beta)*(2*diag(hh)*diag((Dc1*hh).^2)...
                        +2*diag(Dc1*hh)*diag(hh.^2)*Dc1)...hydro2
        -epsilon*1/4*M_c*diag(hh)*diag(Dc2*cc)...   %marangoni1
        -epsilon*1/2*M_c*(diag(Dc1*hh)*diag(Dc1*cc)+...
                          diag(hh)*diag(Dc1*cc)*Dc1) ... %marangoni2
        +1/15*Re*sin(beta)^2*(diag(hh.^6)*Dc2+6*diag(hh.^5)*diag(Dc2*hh))...%inertia1
        +2/5*Re*sin(beta)^2*(2*diag(Dc1*hh)*diag(hh.^5)*Dc1...      %inertia2
                           +5*diag((Dc1*hh).^2)*diag(hh.^4));
    M12 = 1/2*E*K_c*diag(ones(Nx,1),0)...
        -1/2*M_c*diag(hh.^2)*Dc2   ...marangoni1
        -M_c*diag(Dc1*hh)*diag(hh)*Dc1; ...marangoni2;

     %%% c equation

        M21 = diag(-1/2*K_c/Pe^2*cc./hh.^2)+sin(beta)*diag(hh.*(Dc1*cc));
        M22 = 1/dt*diag(ones(Nx,1),0) + diag(1/2*K_c/Pe^2*1./hh) ...
            + 1/6*sin(beta)*diag(hh.^2)*Dc1;
        LM = [M11 M12;
            M21 M22];

        RMh = E*K_c*cc ...   %evaporation
            + sin(beta)*(Dc1*hh).*hh.^2 ... %advection
            +1/3*epsilon*S*hh.^3.*(Dc4*hh)...%cap1
            +epsilon*S*hh.^2.*(Dc3*hh).*(Dc1*hh)... %cap2
            -1/3*epsilon*cos(beta)*hh.^3.*(Dc2*hh)... %hydro1
            -epsilon*cos(beta)*hh.^2.*(Dc1*hh).^2 ... %hydro2
            -1/2*epsilon*M_c*(Dc2*cc).*hh.^2 ...  %marangoni1
            -epsilon*M_c*(Dc1*cc).*hh.*(Dc1*hh) ... %marangoni2
            +2/15*epsilon*Re*sin(beta)^2*(Dc2*hh).*hh.^6 ...  %inertia1
            +4/5*epsilon*Re*sin(beta)^2*(Dc1*hh).^2.*hh.^5;%  ... %inertia2
        RMc =K_c/Pe^2*cc./hh+1/3*sin(beta)*hh.^2.*(Dc1*cc);
```

```
        RM = [RMh ; RMc];

        dHC = -LM\RM;

        HCt2 = HC+dHC;
        hht2 = HCt2(1:Nx);
        cct2 = HCt2(Nx+1:2*Nx);

        %% individual effects
        LMa = 1/dt*diag(ones(Nx,1),0)+1/2*sin(beta)*(diag(hh.^2)...
                *Dc1+diag(hh)*diag(Dc1*hh));
        RMa = sin(beta)*(Dc1*hh).*hh.^2;
        aa = -LMa\RMa;
    if cos(beta)<1e-10
        bb=0*hh;
    else
        LMb = 1/dt*diag(ones(Nx,1),0)-epsilon*1/6*cos(beta)*(diag(hh.^3)*Dc2 ...
              + 3*diag(Dc2*hh)*diag(hh.^2))...
              -epsilon*1/2*cos(beta)*(2*diag(hh)*diag((Dc1*hh).^2)...
              +2*diag(Dc1*hh)*diag(hh.^2)*Dc1);
        RMb = -1/3*epsilon*cos(beta)*hh.^3.*(Dc2*hh)... %
            -epsilon*cos(beta)*hh.^2.*(Dc1*hh).^2;
        bb = -LMb\RMb;
    end
    if S==0
        cch = 0*hh;
    else
        LMch = 1/dt*diag(ones(Nx,1),0)+epsilon*1/6*S*(diag(hh.^3)*Dc4...
            +3*diag(hh.^2)*diag(Dc4*hh))...%cap1
            +epsilon*1/2*S*(diag(hh.^2)*diag(Dc1*hh)*Dc3...     %cap2
            +diag(hh.^2)*diag(Dc3*hh)*Dc1...
            +2*diag(hh)*diag(Dc1*hh)*diag(Dc3*hh));
        RMch = 1/3*epsilon*S*hh.^3.*(Dc4*hh)...%cap1
            +epsilon*S*hh.^2.*(Dc3*hh).*(Dc1*hh);
        cch = -LMch\RMch;
    end

        eev = -E*K_c * cc;

    H(:,i+1) = hht2;
    C(:,i+1) = cct2;
    A(:,i) = aa;
    B(:,i) = bb;
    Ch(:,i) = cch;
    Ev(:,i) = eev;

end
film=H;
conc=C;

end
```

B.2 Forward Euler Solver

```
function [film conc]= forward()

% this is a function that solves the simple film equation for beta = 0
% h_t + A(h)*h_x +eps*(B(h)*h_x + C(h)*h_{xxx})_x = 0
% where A(h) = sin(beta)*h^2, B(h) = -h^3/3, C(h) = S*h^3/3
% on 0 < x < 2\pi, periodic boundary conditions in x
% using forward Euler

global E K_c M_c epsilon beta Re S k Nx xend dx dt tend tsize x H C Pe

% set up spatial differentiation matrices
%%%% first derivative
Dc1 = diag(ones(Nx-1,1),1)+diag(-ones(Nx-1,1),-1);%%%central
Dc1(1,end) = -1; Dc1(end,1) = 1;
Dc1 = 1/2/dx*Dc1;

%%%% second derivative
Dc2 = diag(ones(Nx-1,1),1) + diag(-2*ones(Nx,1))+diag(ones(Nx-1,1),-1);
Dc2(1,end) = 1; Dc2(end,1) = 1;
Dc2 = 1/dx^2*Dc2;

%%%% third derivatve
Dc3 = diag(ones(Nx-2,1),2) - diag(2*ones(Nx-1,1),1)...
    +diag(2*ones(Nx-1,1),-1)-diag(ones(Nx-2,1),-2);
Dc3(1,end-1:end)=[-1 2]; Dc3(2,end) = -1;
Dc3(end-1:end,1)=[1 -2]; Dc3(end,2) = 1;
Dc3 = 1/2/dx^3*Dc3;

%%%% fourth derivative
Dc4 = diag(ones(Nx-2,1),2)+diag(-4*ones(Nx-1,1),1)...
    +diag(6*ones(Nx,1)) +diag(-4*ones(Nx-1,1),-1)...
    +diag(ones(Nx-2,1),-2);
Dc4(1,end-1:end) = [1 -4]; Dc4(2,end)=1;
Dc4(end-1:end,1) = [1 -4]; Dc4(end,2)=1;
Dc4 = 1/dx^4*Dc4;

% start time iteration

for i = 1:tsize %t = dt:dt:tend %
    %
    % go through iterates
    %
    h0 = H(:,i);c0=C(:,i);
    h0x = Dc1*h0; h0xx = Dc2*h0; h0xxx=Dc3*h0; h0xxxx = Dc4*h0;

    c0x=Dc1*c0;c0xx=Dc2*c0;
```

```
    rhs = sin(beta)*h0.^2.*h0x +E*K_c*c0+ epsilon*(...
        +1/3*S.*(h0.^3.*h0xxxx+3*h0.^2.*h0x.*h0xxx)...
        +2/15*Re*sin(beta)^2*(h0.^6.*h0xx+h0.^5.*h0x.^2)...
        -1/3*cos(beta)*(h0.^3.*h0xx+3*h0.^2.*h0x.^2)...
        -1/2*M_c.*(c0x.*2.*h0.*h0x+c0xx.*h0.^2));

    H(:,i+1) = H(:,i) - dt*rhs;

    rhsc = 1/3*sin(beta)*h0.^2.*c0x+K_c/E/Pe^2*c0./h0;

    C(:,i+1) = C(:,i) - dt*rhsc;

end

film=H;
conc=C;
```

B.3 Data Analysis and Plots Generation

B.3.1 Run and Catch Result

```
[r11 r12 A B Ch Ev debug]= main(4);
```

B.3.2 Time and space plots

```
subplot(1,2,1)
mesh(t,x,r11);
set(ylabel('x'),'fontsize',20);
set(xlabel('time'),'fontsize',20);
set(zlabel('Height'),'fontsize',20);
set(title('Height in Space and Time','fontsize',20));
subplot(1,2,2)
mesh(t,x,r12);
set(ylabel('x'),'fontsize',20);
set(xlabel('time'),'fontsize',20);
set(zlabel('Concentration'),'fontsize',20);
set(title('Concentration in Space and Time','fontsize',20));

subplot(2,2,3)
plot(t,max(r11)-min(r11))

subplot(2,2,4)
plot(t,max(r12))
```

B.3.3 Plot of The Peak Shift

```
set(figure(1),'position',[176    51   603   760])
a = size(r11);

aa1= 1;
aa= a(2);

pp =zeros(2,aa-aa1); %peak positions
for i =1:(aa-aa1-1)

    ph = find(r11(:,i+aa1)==max(r11(:,i+aa1)),1,'first');
    pc = find(r12(:,i+aa1)==max(r12(:,i+aa1)),1,'first');
    dd = (ph -pc)*dx;

    if (dd<0 && dd>-xend)
        dd = dd+xend;
    end



    pp(:,i) = dx*[ph pc]';
end
ttt = aa1*dt:dt:dt*aa-dt;

subplot(3,1,1)
plot(ttt,max(r11(:,aa1:aa-1))-min(r11(:,aa1:aa-1)),'LineWidth',2,'Color','black')
xlim([aa1*dt aa*dt])
set(xlabel('Time'),'fontsize',20);
set(ylabel('\Deltax'),'fontsize',20);


subplot(3,1,2)
plot(ttt,pp(1,:),'LineWidth',2,'Color','blue');hold on
plot(ttt,pp(2,:),'LineWidth',2,'Color','red');

leg=legend('Film','Concentration');
set(leg,'fontsize',20,'position',[0.6089    0.5672    0.3781    0.0974])
set(xlabel('Time'),'fontsize',20);

set(ylabel('x position','fontsize',20));
xlim([aa1*dt aa*dt])
subplot(3,1,3)
plot([0 ttt],(max(r12)-min(r12))/2,'LineWidth',2)
set(xlabel('Time'),'fontsize',20);
set(ylabel('Amplitude'),'fontsize',20);
xlim([0 aa*dt])

allAxes = findall(0,'type','axes');
set(allAxes,'fontsize',20);
```

B.3.4 Profile plot of the peak shift

```
figure(2)
set(figure(2),   'position', [411    292   1200   520])

ti = [26 0.3 27.5];
taa = ti(1)/dt:ti(2)/dt:ti(3)/dt;
ta=taa*dt;

ab=subplot(1,2,1);set(ab,'position',[0.1300    0.1476    0.3347    0.7774])
plot(x,r11(:,taa)-1,'LineWidth',2);
set(xlabel('x'),'fontsize',22);
set(ylabel('Film Profile'),'fontsize',22);


axis([0 (xend-dx) 1.1*min(min(r11(:,taa)-1)) 1.01*max(max(r11(:,taa)-1)) ])

subplot(1,2,2)
plot(x,r12(:,taa),'LineWidth',2)
set(xlabel('x'),'fontsize',22);
set(ylabel('Concentration Profile'),'fontsize',22);

xlim([0 xend-dx])
ll = legend(strcat('t=',num2str(ta(1))),...
    strcat('t=',num2str(ta(2))),...
    strcat('t=',num2str(ta(3))),...
    strcat('t=',num2str(ta(4))),...
    strcat('t=',num2str(ta(5))),...
    strcat('t=',num2str(ta(6))));%,...
set(ll,'fontsize',22,'position',[0.8521 0.4674 0.1287  0.5063])

allAxes = findall(0,'type','axes');
set(allAxes,'fontsize',22);
```

B.3.5 Different Effects Plot

```
figure(5)

set(figure(5),   'position', [130  156  913  618])
subplot(2,2,1)
plot(x,A(:,taa),'LineWidth',2)
set(xlabel('x'),'fontsize',18);
set(ylabel('Wave propagation'),'fontsize',18);
xlim([0 xend-dx])

subplot(2,2,2)
plot(x,B(:,taa),'LineWidth',2)
set(xlabel('x'),'fontsize',18);
```

```
set(ylabel('Hydrostatic'),'fontsize',18);
xlim([0 xend-dx])

subplot(2,2,3)
plot(x,Ch(:,taa),'LineWidth',2)
set(xlabel('x'),'fontsize',18);
set(ylabel('Capillary'),'fontsize',18);
xlim([0 xend-dx])

subplot(2,2,4)
plot(x,Ev(:,taa),'LineWidth',2)
set(xlabel('x'),'fontsize',18);
set(ylabel('Evaporation'),'fontsize',18);
xlim([0 xend-dx])

allAxes = findall(0,'type','axes');
set(allAxes,'fontsize',20);
```

Appendix C

Plots with Different Parameter values

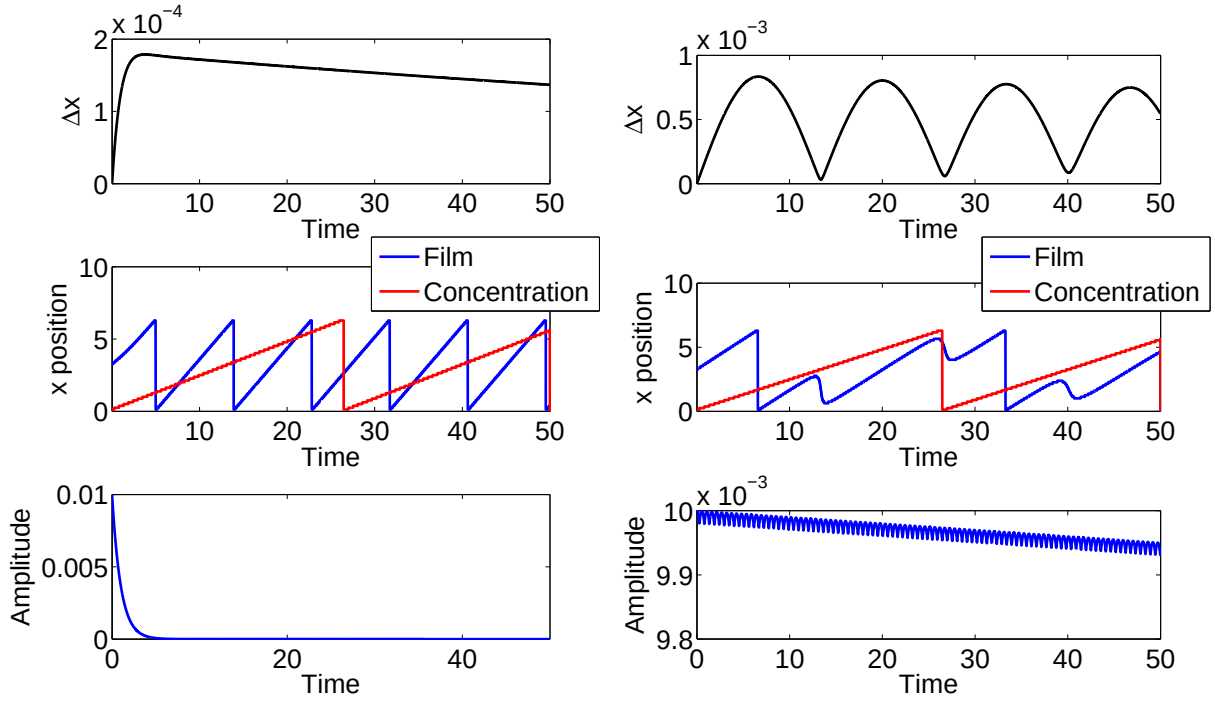

Figure C.1: Left plots are when $Pe = 0.1$ and right $Pe = 10$. Other Parameter values are: $S = 1$, $\beta = \pi/4$, $M = Re = 0$, $E = 1$, $K_c = 0.01$.

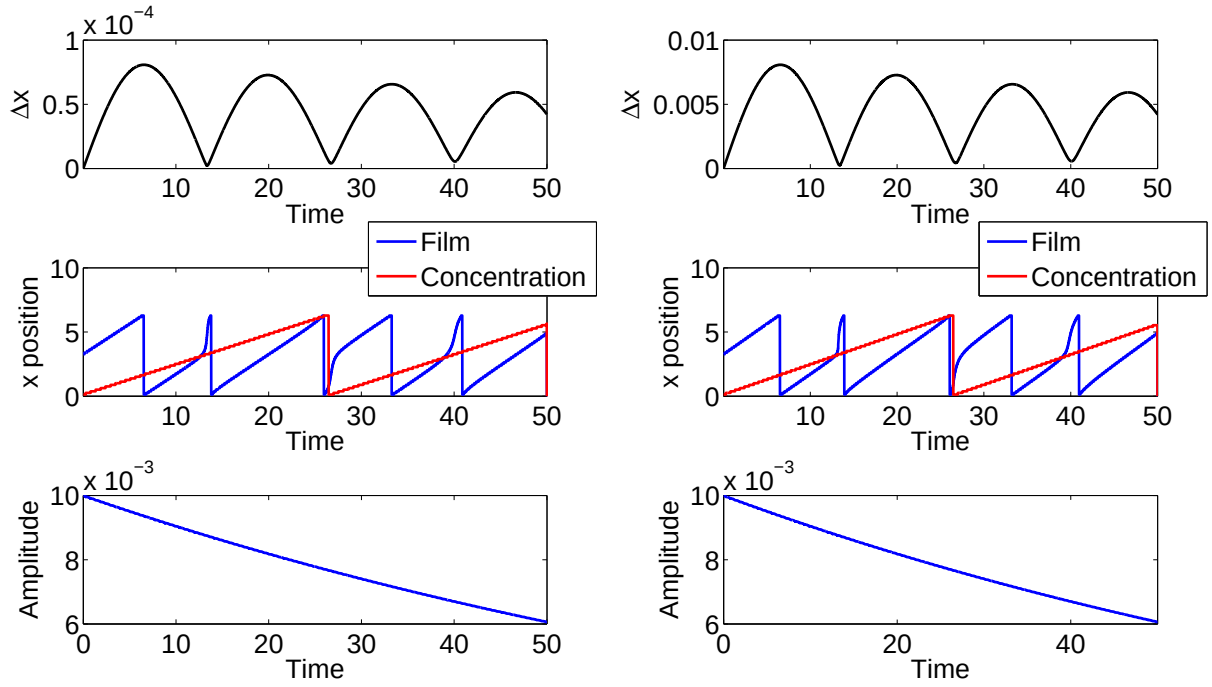

Figure C.2: Left plots are when $E = 0.1$ and right $E = 10$. Other Parameter values are: $\beta = \pi/4$, $Pe = 1$, $S = 1$, $M = Re = 0$, $K_c = 0.01$.

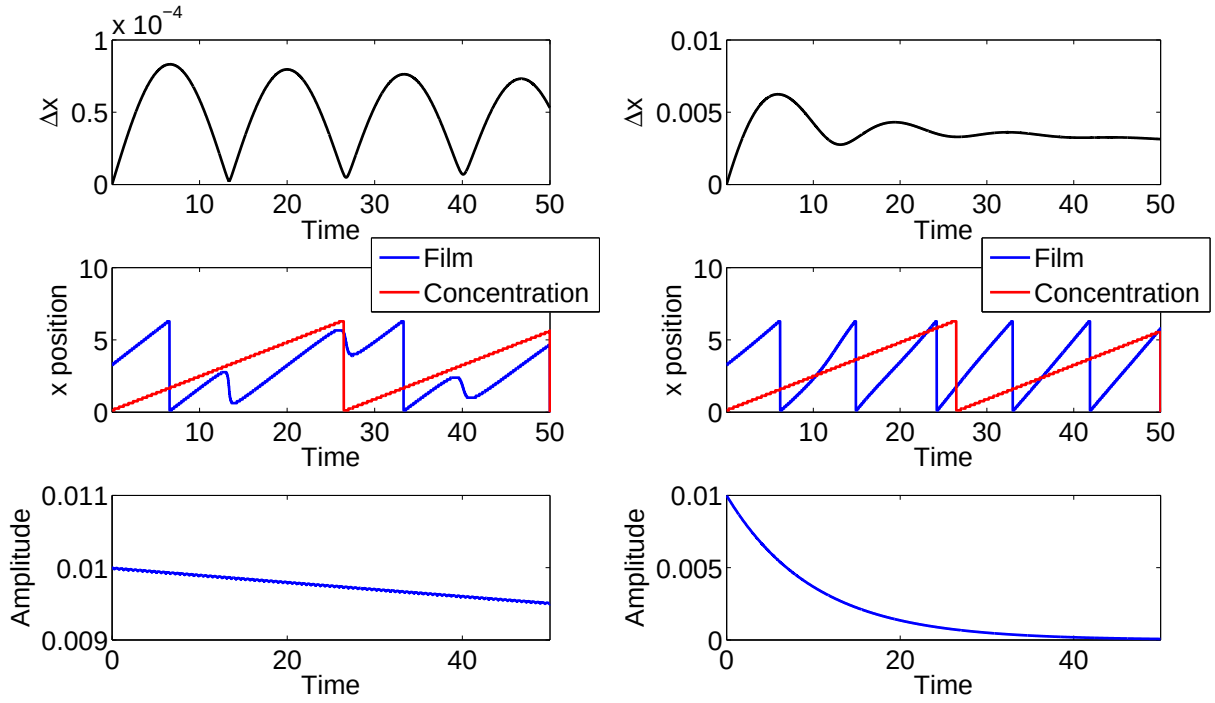

Figure C.3: Left plots are when $K_c = 0.001$ and right $K_c = 0.1$. Other Parameter values are: $\beta = \pi/2$, $Pe = 1$, $M = Re = 0$, $E = 1$, $S = 1$.

Appendix D

Plots compare

We will compare four sets of parameters values respectively:

- $C = 0.05\cos(kx)$ and $M = 0$
- $C = 0.05\cos(kx)$ and $M = 1$
- $C = 0.1\cos(kx)$ and $M = 0$
- $C = 0.1\cos(kx)$ and $M = 1$

The plots will be appearing in the order of the above list. Upper left being the first set, upper right the second, lower left the third and lower right the fourth set.

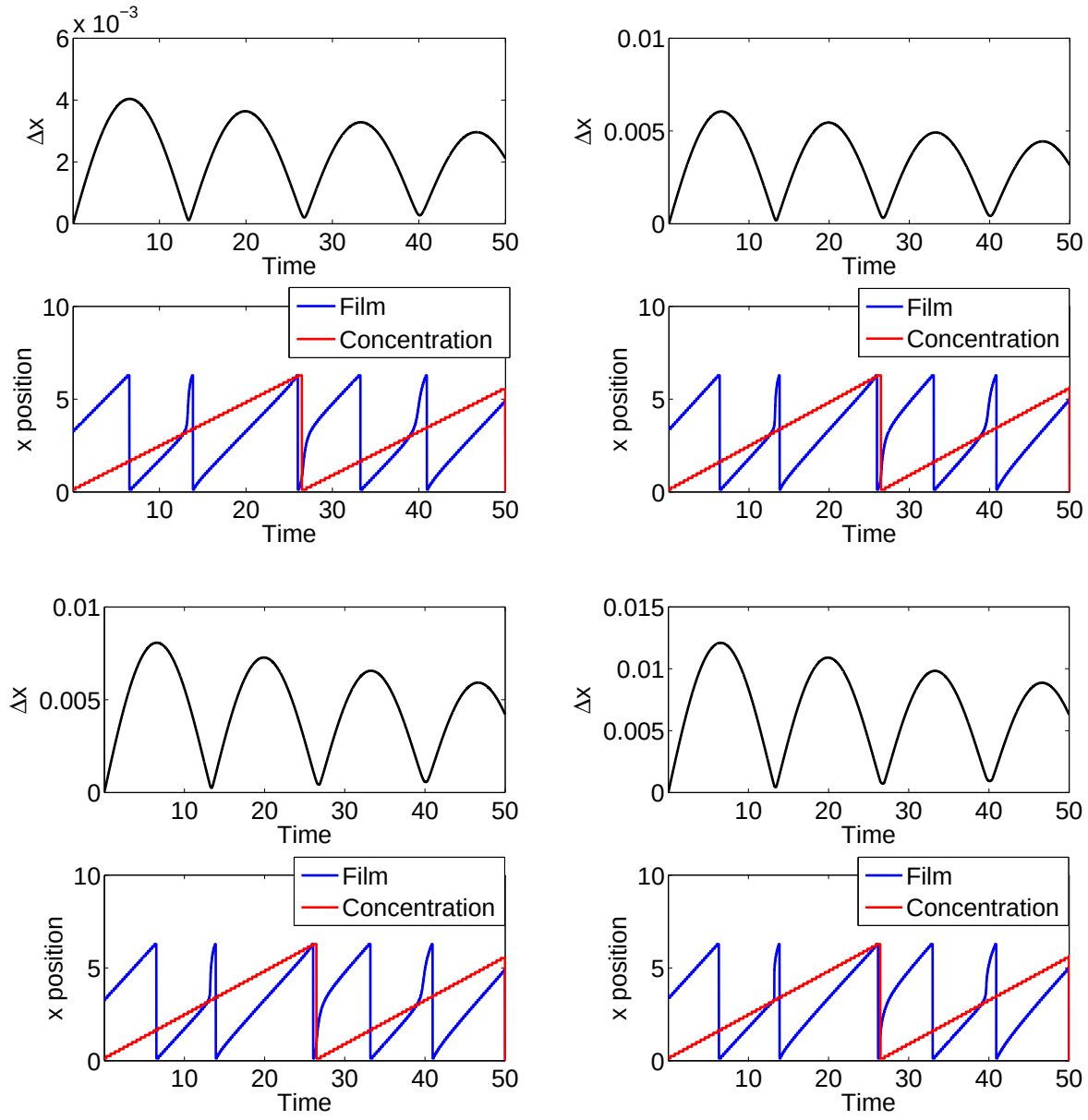

Figure D.1: Other parameter values are: $S = 1$, $Pe = 1$, $\beta = \pi/4$, $E = 1$, $K_c = 0.01$, $Re = 0$, and $\varepsilon = 0.01$

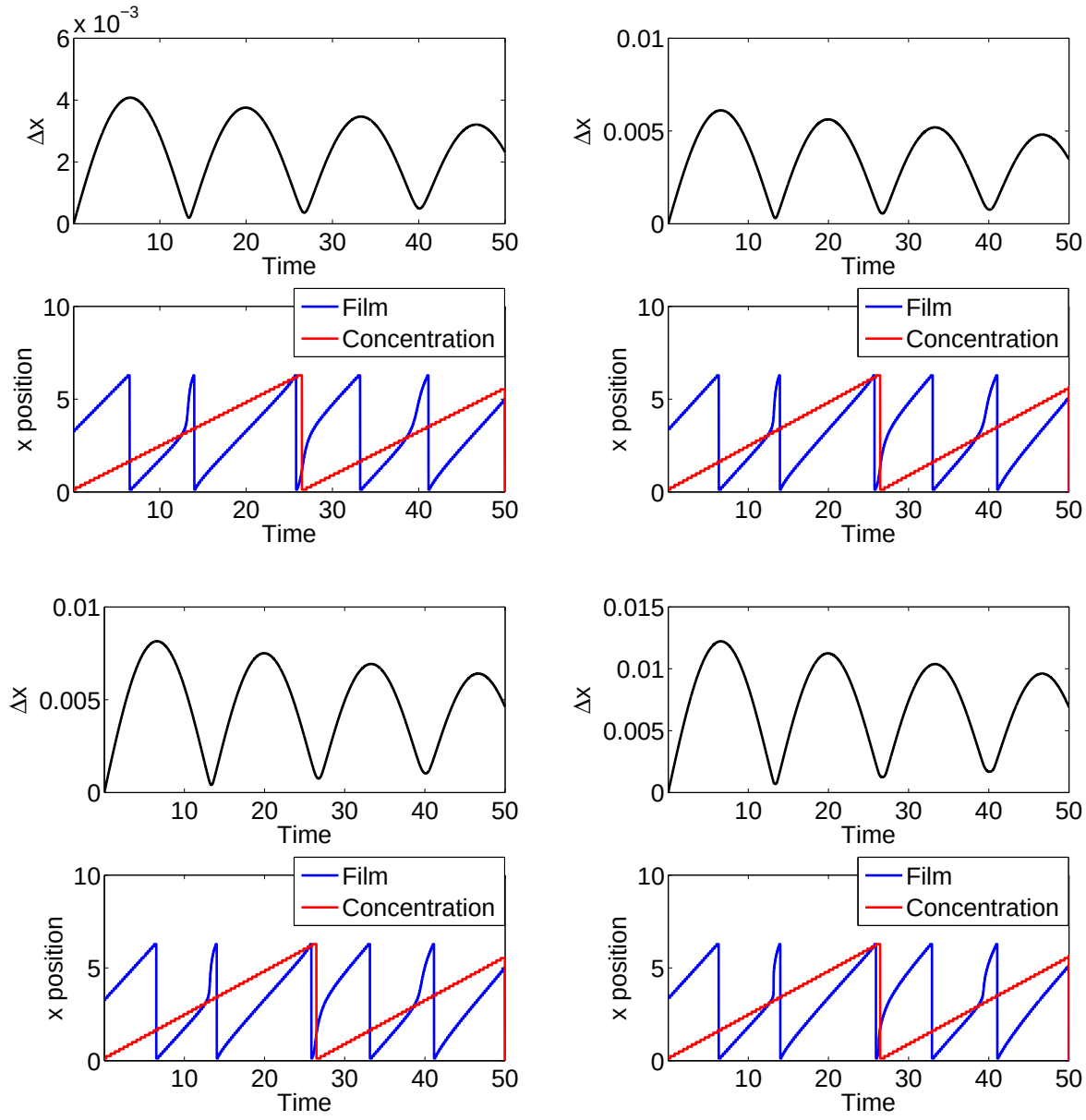

Figure D.2: Other parameter values are: $S = 0.1$, $Pe = 1$, $\beta = \pi/4$, $E = 1$, $K_c = 0.01$, $Re = 0$, and $\varepsilon = 0.01$

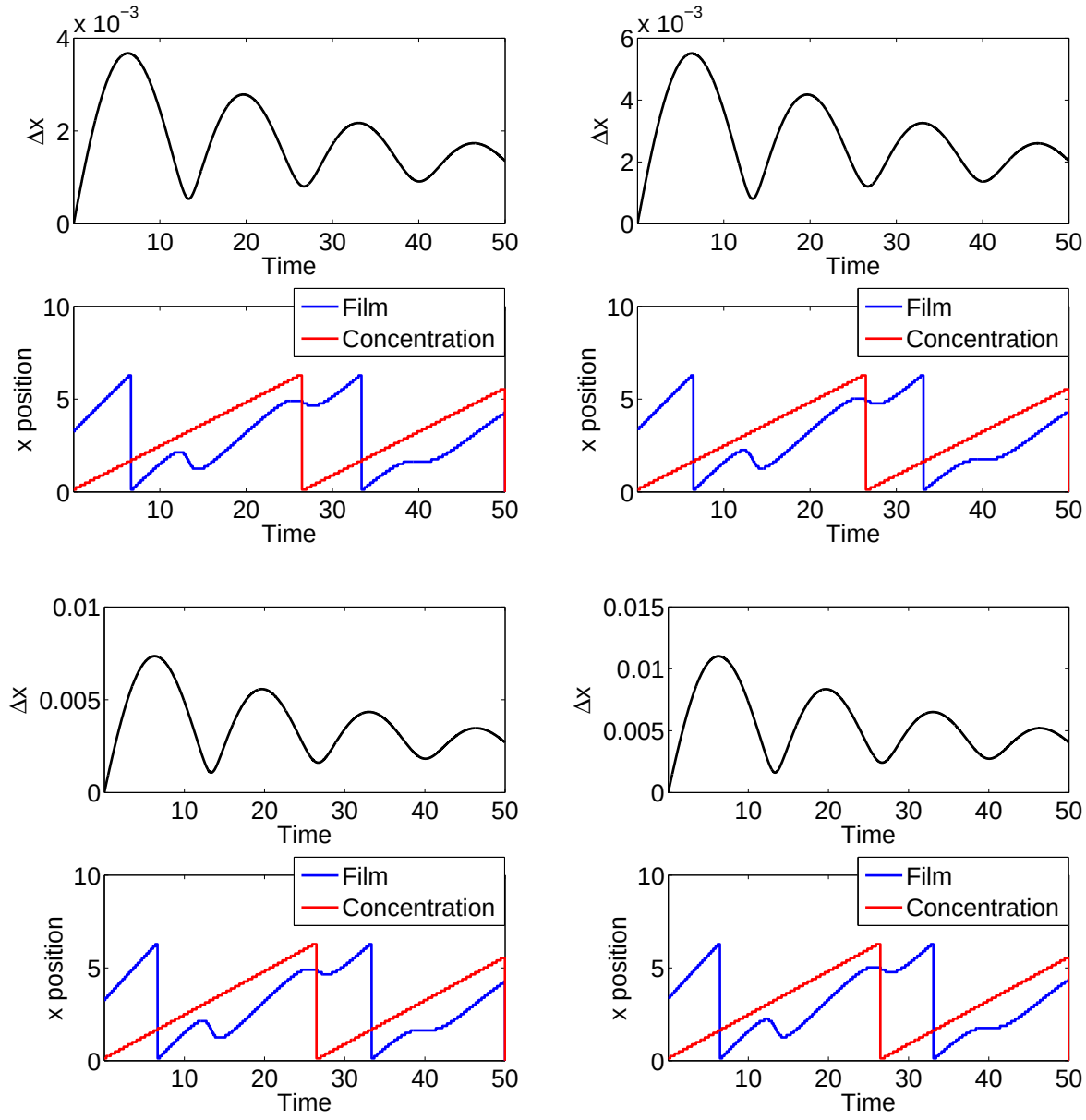

Figure D.3: Other parameter values are: $S = 10$, $Pe = 1$, $\beta = \pi/4$, $E = 1$, $K_c = 0.01$, $Re = 0$, and $\varepsilon = 0.01$

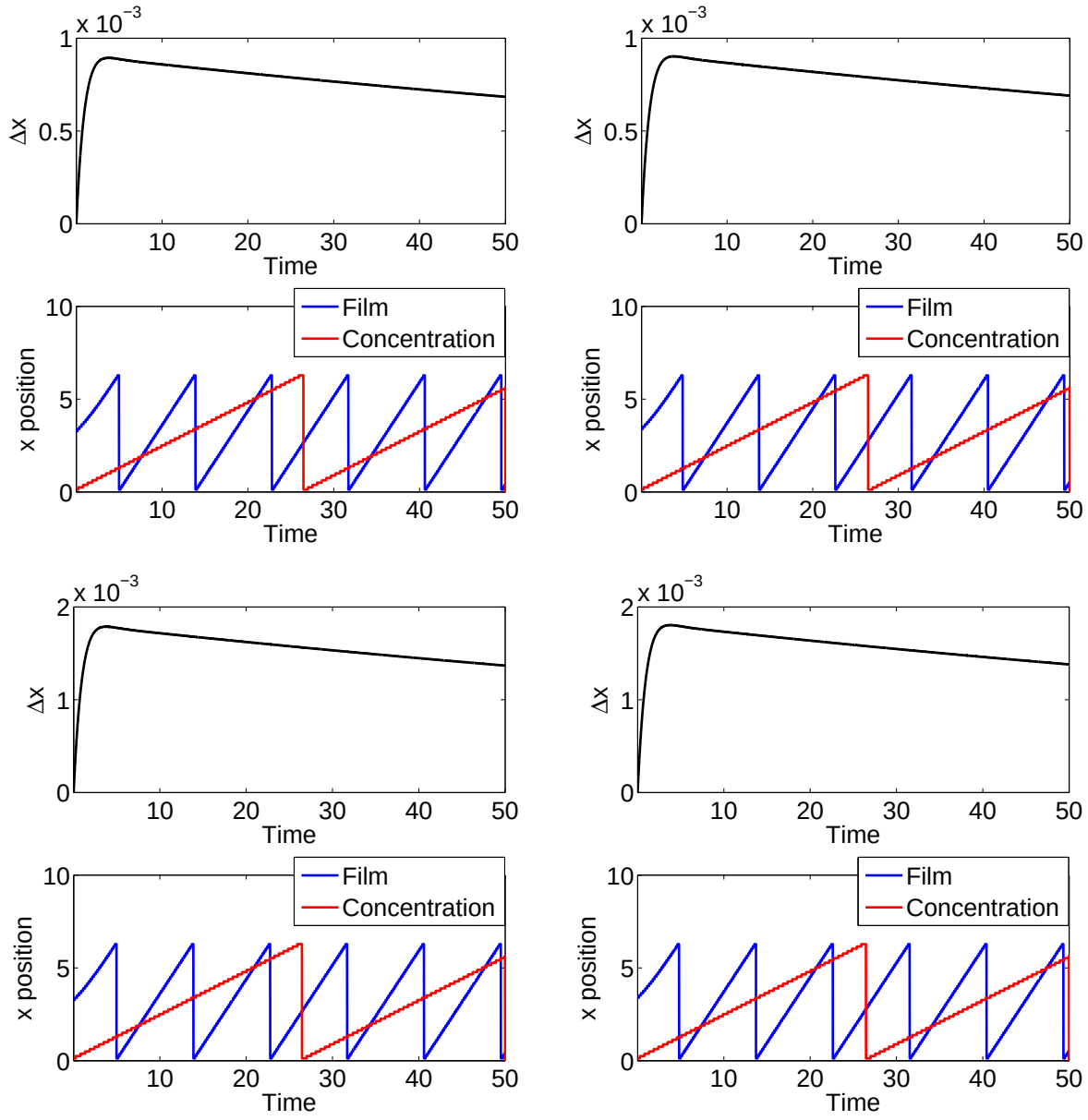

Figure D.4: Other parameter values are: $S = 1$, $Pe = 0.1$, $\beta = \pi/4$, $E = 1$, $K_c = 0.01$, $Re = 0$, and $\varepsilon = 0.01$

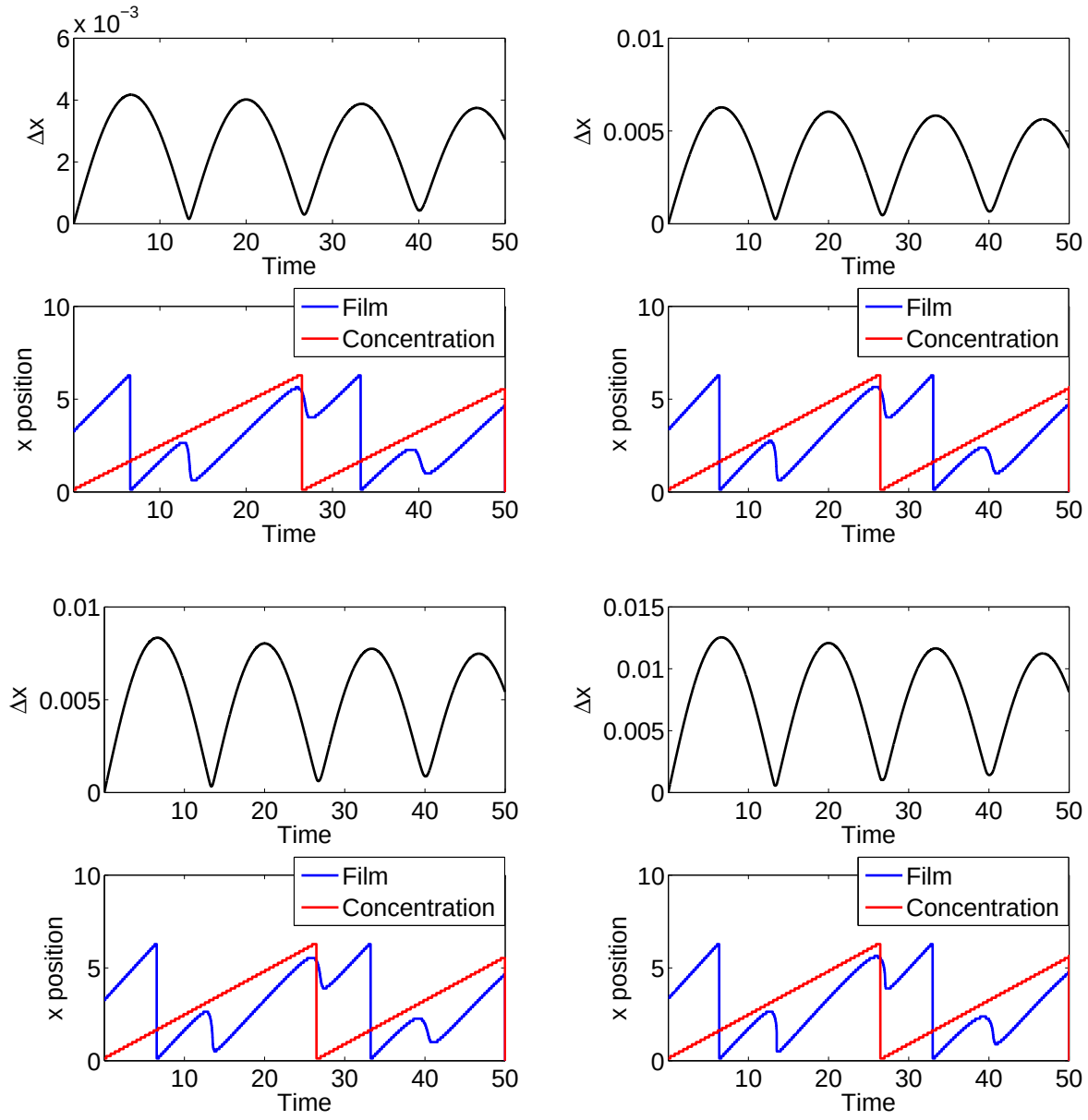

Figure D.5: Other parameter values are: $S = 1$, $Pe = 10$, $\beta = \pi/4$, $E = 1$, $K_c = 0.01$, $Re = 0$, and $\varepsilon = 0.01$

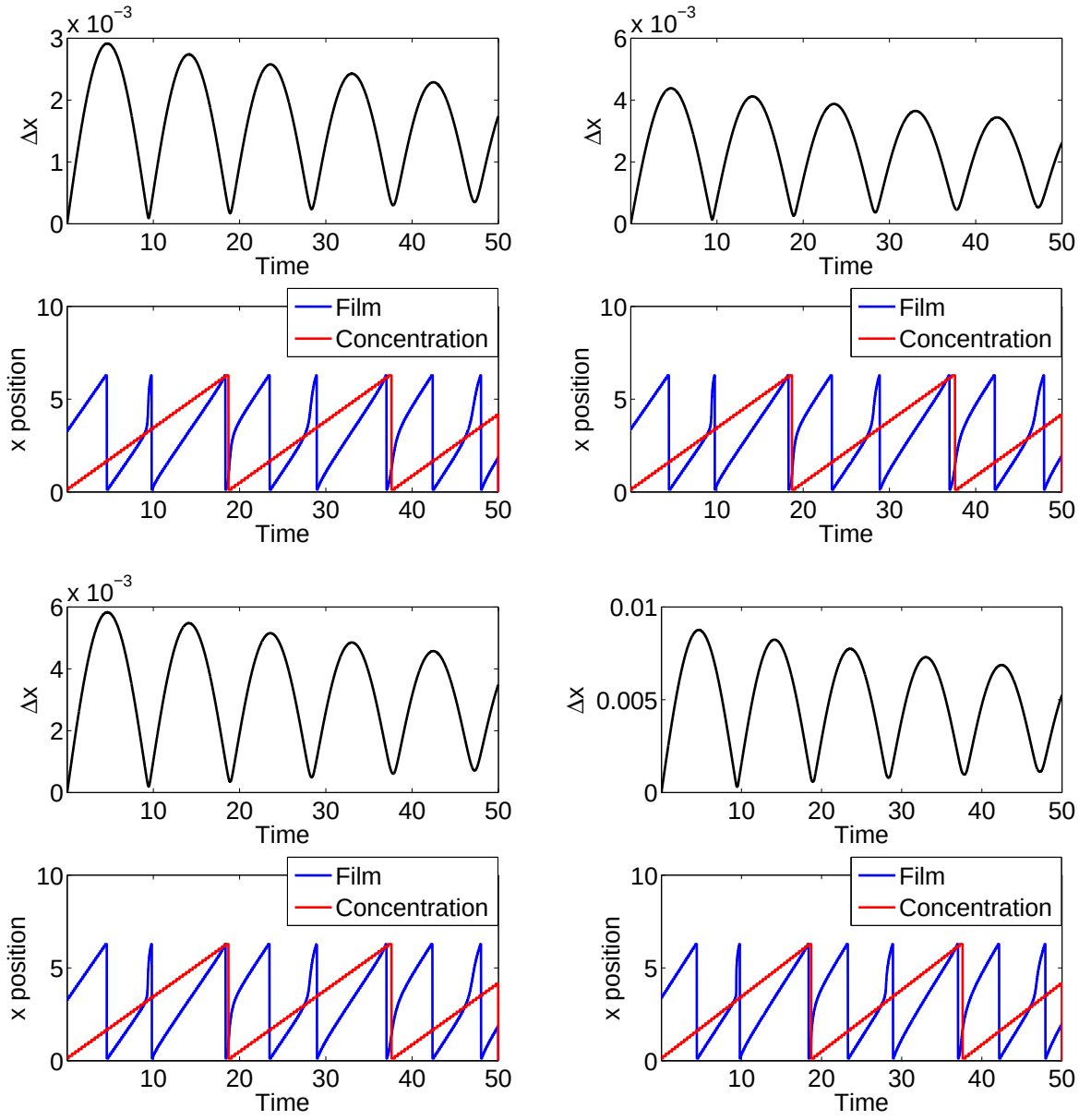

Figure D.6: Other parameter values are: $S = 1$, $Pe = 1$, $\beta = \pi/2$, $E = 1$, $K_c = 0.01$, $Re = 0$, and $\varepsilon = 0.01$

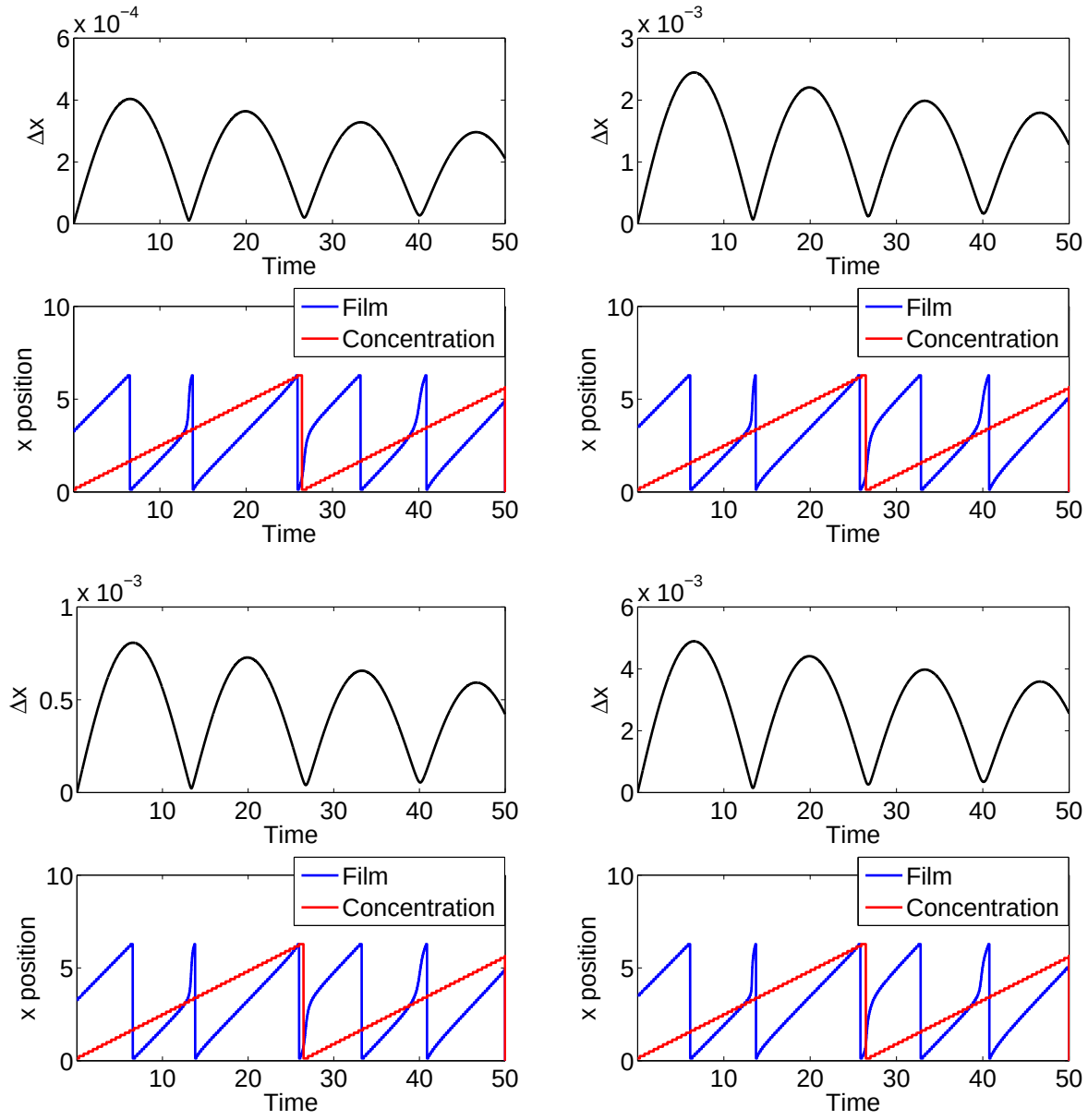

Figure D.7: Other parameter values are: $S = 1$, $Pe = 1$, $\beta = \pi/4$, $E = 0.1$, $K_c = 0.01$, $Re = 0$, and $\varepsilon = 0.01$

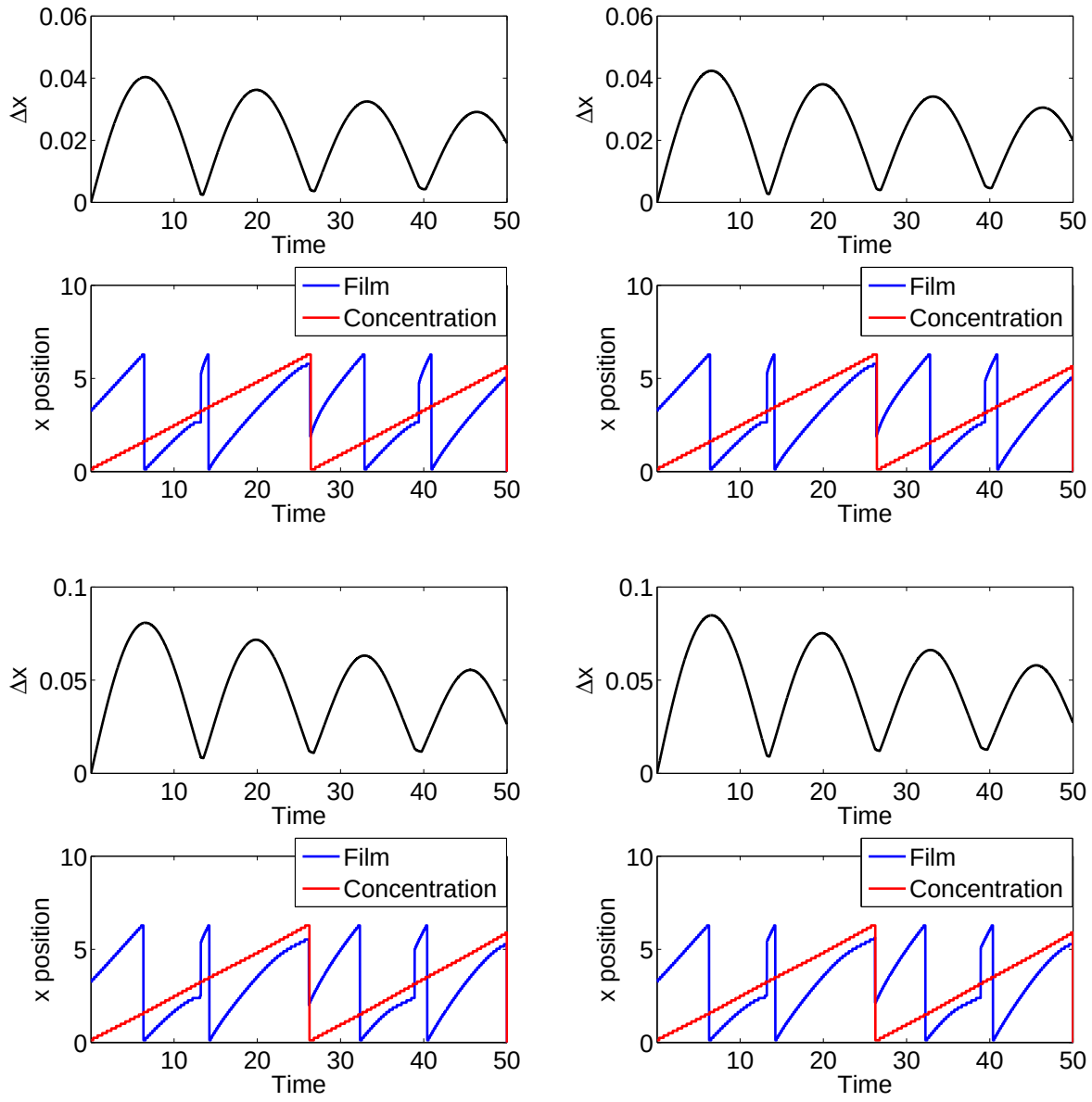

Figure D.8: Other parameter values are: $S = 1$, $Pe = 1$, $\beta = \pi/4$, $E = 10$, $K_c = 0.01$, $Re = 0$, and $\varepsilon = 0.01$

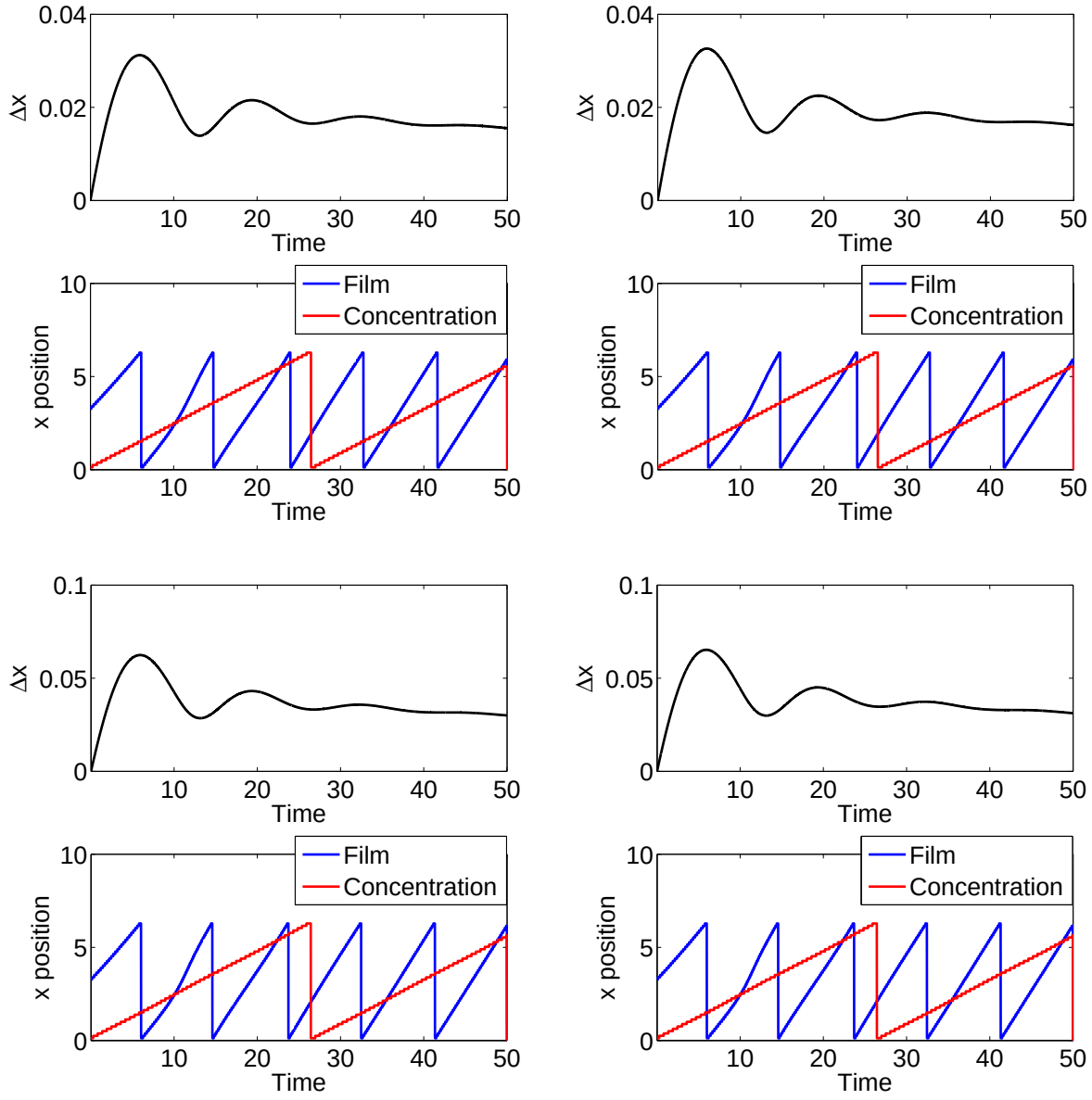

Figure D.9: Other parameter values are: $S = 1$, $Pe = 1$, $\beta = \pi/4$, $E = 1$, $K_c = 0.1$, $Re = 0$, and $\varepsilon = 0.01$

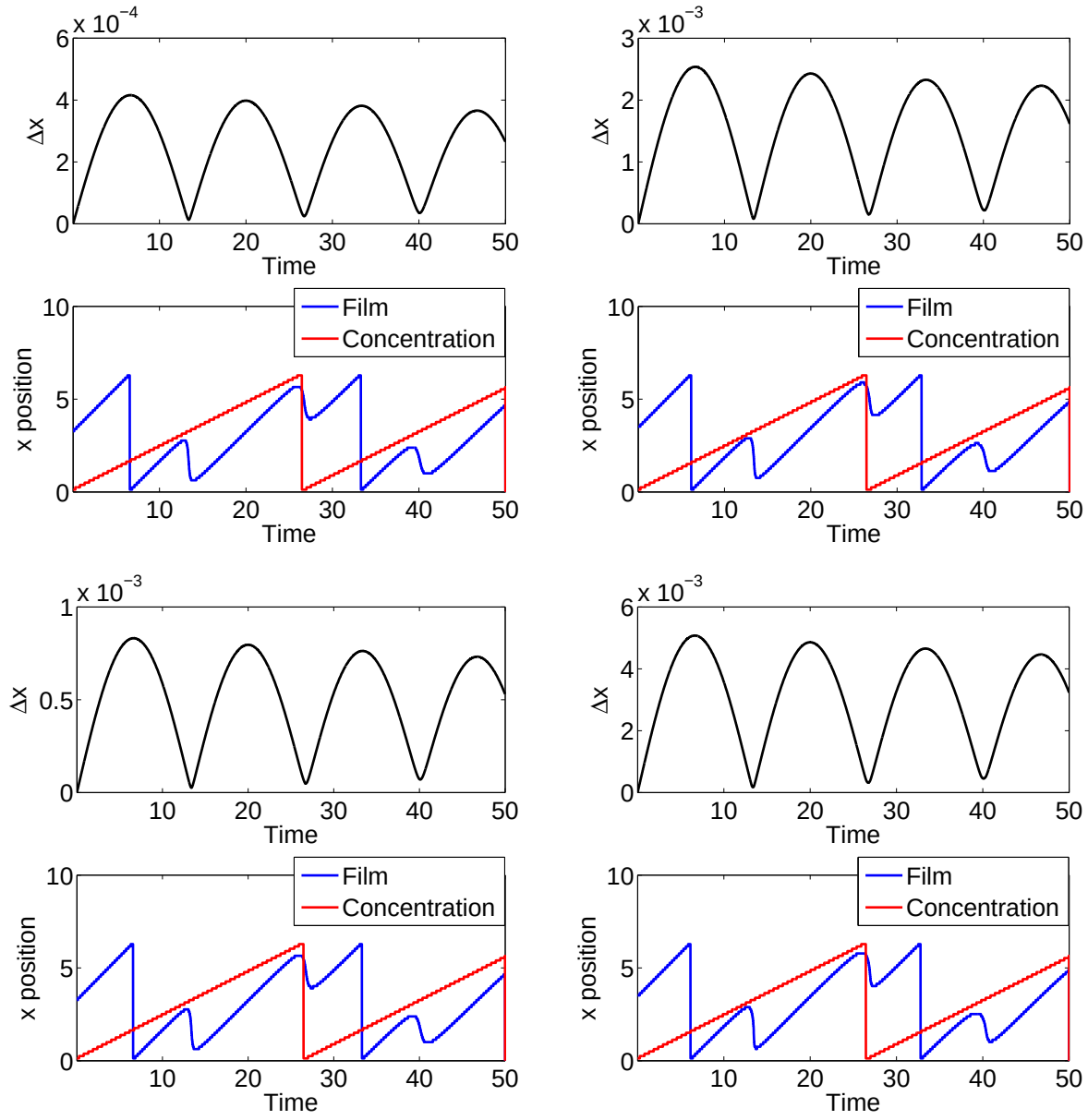

Figure D.10: Other parameter values are: $S = 1$, $Pe = 1$, $\beta = \pi/4$, $E = 1$, $K_c = 0.001$, $Re = 0$, and $\varepsilon = 0.01$

Bibliography

[1] H. E. Huppert and J. E. Simpson. The slumping of gravity currents. *J. Fluid Mech.*, 99:785–799, 1980.

[2] I. Fatt H. Wong and C. J. Radke. Deposition and thinning of the human tear film. *J. Colloid and Interface Science*, 184(0595):44–51, 1996.

[3] G. K. Batchelor. *An Introduction to Fluid Dynamics*. Cambridge University Press, 2000.

[4] K. R. Thomas. *Physical Phenomena of Thin Surface Layers*. PhD thesis, University of Cambridge, 2010.

[5] S. H. Davs A. Oron and S. G. Bankoff. Long-scale evolution of thin liquid films. *Reviews of Modern Physics*, 69(3):931–980, 1997.

[6] U. Thiele J. M. Skotheim and B. Scheid. On the instability of a falling film due to localized heating. *J. Fluid Mech*, 475:1–19, 2003.

[7] B. Scheid. *Evolution and stability of falling liquid films with thermocapillary effects*. PhD thesis, University of Bruxelles, 2004.

[8] D. J. Benney. Long wave on liquid films. *J. Fluid Mech.*, 45:150–155, 1966.

[9] R. J. Roskes. Three-dimensional long waves on a liquid film. *Phys. Fluids*, 13:1440–1445, 1970.

[10] S. P. Lin and M. V. G. Krishna. Stability of a liquid film with respect to initially finite three-dimensional disturbances. *Phys. Fluids*, 20:2005–2011, 2005.

[11] J. G. Schneider J. Liu and J. P. Gollub. Three-dimensional instabilities of film flows. *Fhys. Fluids*, 7(1):55–67, 1994.

[12] S. H. Davis J. P. Burelbach, S. G. Bankoff. Nonlinear stability of evaporating/condensing liquid films. *J. Fluid Mech.*, 195, 1988.

[13] A. E. Hosoi and J. W. M. Bush. Evaporative instabilities in climbing films. *J. Fluid Mech*, 442:217–239, 2001.

[14] M. Hennenberg B. Weyssow S. Slavtchev and B. Scheid. Coupling between stationary Marangoni and Cowley-Rosensweig instabilities in a deformable ferrofluid layer. 1(1), 2007.

[15] D. Takagi and H. E. Huppert. Flow and instability of thin films on a cylinder and sphere. *J. Fluid mech.*

[16] L. D. Landau and E. M. Lifshitz. *Fluid Mechanics*. Course of Theoretical Physics. Pergamon Press, thrid edition, 1966.

[17] P. Nithiarasu R. W. Lewis and K. N. Seetharamu. *Fundamentals of the Finite Element Method for Heat and Fluid Flow*. Wiley, 2004.

[18] E. Alvarez G. Vhquez and J. M. Navaza. Surface tension of alcohol + water from 20 to 50 ”c. *J. Chem. Eng. Data*, pages 611–614, 1995.

[19] A. E. Hosoi L. Kondic Z. Borden, H. Grandjean and B. S. Tilley. Instabilities and taylor dispersion in isothermal binary thin fluid films. *Phys. Fluids*, 20, 2008.

[20] P. G. Drazin and W. H. Reid. *Hydrodynamic Stability*. Cambridge University Press, second edition, 2004.

[21] H. J. Palmer. The hydrodynamics stability of rapidly evaporating liquids at reduced pressure. *J. Fluid Mech.*, 75:487–511, 1976.

[22] S. G. Bankoff S. W. Joo, S. H. Davis. Long-wave instabilities of heated falling films: Two-dimensional theory of uniform layers. *J. Fluid Mech.*, 230:117–146, 1991.

[23] V. A. Bloomfield and R. K. Dewan. Viscosity of liquid mixtures. *J. Phys. Chem.*, 75(20):3113–3119, 1956.

[24] J. Chipman. *The Soret Effect*. PhD thesis, University of California, 1926.

[25] H. Raszillier K. D. Danova, N. Alleborn and F. Durst. The stability of evaporating thin liquid films in the presence of surfactant.I. lubrication approximation and linear analysis. *Phys. Fluids*, 10:131–143, 1998.

[26] M. G. Velarde E. A. Demekhin, S. Kalliadasis. Suppressing falling film instabilities by Marangoni forces. *Phys. Fluids*, 18, 2006.

[27] G. M. Homsy. Combined buoyancy-termocapillary convection. Technical report, Standford University, 1991.

[28] O. E. Jensen and J. B. Grotberg. The spreading of heat or soluble surfactant along a thin liquid film. *Phys. Fluids*, 5:58–68, 1993.

[29] T. Ree S. W. Kim, M. S. Jhon and H. Eyring. The surface tension of binary liquid mixtures. 1967.

[30] J. Lowengrub; L. Truskinovsky. Quasi-incompressible Cahn-Hilliard fluids and topological transitions. *Proceedings: Mathematical, Physical and Engineering Sciences*, 454(1978):2617–2654.

[31] O. K. Matar and P. D. M. Spelt. Dynamics of thin free films with reaction-driven density and viscosity variations. *Phys. Fluids*, 17, 2005.

[32] G. Lebon S. Miladinova, D. Staykova and B. Scheid. Effect of nonuniform wall heating on the three-dimensional secondary instability of falling films. 2002.

[33] A. Oron and A. A. Nepomnyashchy. Long-wavelength thermocapillary instability with the soret effect. *Physical Review E*, 69, 2004.

[34] L. Rongy and A. De Wit. Buoyancy-driven convection around exothermic autocatalytic chemical fronts traveling horizontally in covered thin solution layers. *J. Chem. Phys.*, 131, 2009.

[35] A. Oron P. Rosenau and J. M. Hyman. Bounded and unbounded patterns of the benney equation. *Phys. Fluids*, 4(8):1102–1104.

[36] B. Scheid, S. Kalliadasis, C. Ruyer-Quil, and P. Colinet. Interaction of three-dimensional hydrodynamic and thermocapillary instabilities in film flows. *Phys. Rev. E*, 78, Dec 2008.